Molecular Therapy
Nucleic Acids
Original Article

Mbd2 Mediates Retinal Cell Apoptosis by Targeting the lncRNA Mbd2-AL1/miR-188-3p/Traf3 Axis in Ischemia/Reperfusion Injury

Yanni Ge,[1,2] Ran Zhang,[1,2] Yuqing Feng,[1,2] and Huiling Li[1,2]

[1]Department of Ophthalmology in the Second Xiangya Hospital, Central South University, Changsha, 410011 Hunan, China; [2]Hunan Clinical Research Center of Ophthalmic Disease, Changsha, 410011 Hunan, China

Recent studies reported that DNA methylation was involved in retinal cell death. Methyl-CpG binding domain protein 2 (Mbd2) is one of the DNA methylation readers. Its role and mechanism of regulation remain unclear. The ischemia/reperfusion (I/R) model in mice primary culture retinal ganglion cells (RGCs) and Mbd2 knockout (Mbd2-KO) mice was used in the current study. We demonstrated that Mbd2 mediates RGC apoptosis caused by I/R injury. Mechanistically, the data suggested that Mbd2 upregulated Mbd2-associated long noncoding RNA 1 (Mbd2-AL1) via demethylation of its promoter. Furthermore, Mbd2-AL1 sponged microRNA (miR)-188-3p, thus preventing tumor necrosis factor (TNF) receptor-associated factor 3 (Traf3) downregulation and inducing RGC apoptosis. This was further demonstrated by the fact that inhibition of miR-188-3p diminished the anti-apoptosis role of Mbd2-AL1 small interfering RNA (siRNA). Finally, it showed that the apoptosis of retinal cells was attenuated, and the visual function was preserved in Mbd2-KO mice, which were associated with the Mbd2-AL1/miR-188-3p/Traf3 axis. Our present study revealed the role of Mbd2 in RGC apoptosis, which may provide a novel therapeutic strategy for retinal ischemic diseases.

INTRODUCTION

Retinal ischemia/reperfusion (I/R) injury is a common cause of irreversible visual impairment that is associated with glaucoma, diabetic retinopathy, and retinal vascular occlusive disorders,[1,2] and leads to blindness, affecting over 100 million individuals in the world. The key reason is the lack of a relatively effective treatment. Previous studies demonstrated that the apoptosis of retinal ganglion cells (RGCs) caused by the endoplasmic reticulum, oxidative stress, and mitochondrial dysfunction played a pivotal role in retinal ischemia injury.[3–5] Interestingly, recent studies have reported that DNA methylation, one of the main mechanisms of epigenetic modification, was involved in the regulation of gene transcription in various diseases, including retinal cell death.[6–10] Methyl-CpG binding domain protein 2 (Mbd2), a key member of methyl-CpG-binding domain proteins (MBDs), plays an essential role in DNA methylation.[7,11] Furthermore, two studies suggested the involvement of Mbd2 in apoptosis of muscle cells caused by ischemic injury[12] and in apoptosis of renal cells that are induced by vancomycin.[10] So far, the role and molecular mechanism of Mbd2 in RGC apoptosis following retinal I/R injury remain unclear.

Recently, long noncoding RNAs (lncRNAs) that are nonprotein-coding transcripts containing more than 200 nucleotides have been shown to mediate several biological processes, such as cell differentiation, metastasis, proliferation, and apoptosis.[13–15] Furthermore, lncRNAs play important roles in human disorders, including stressed RGCs.[16] MicroRNAs (miRNAs) have also been shown to regulate proliferation and apoptosis.[17] Usually, lncRNA-miRNA interactions were considered as competing endogenous RNAs (ceRNAs) that regulate the expression of target genes.[18,19] Although previous studies have suggested the direct involvement of Mbd2 in the regulation of miRNAs,[10] it is unclear whether Mbd2 mediates I/R-induced RGC apoptosis via its interaction with lncRNAs.

In the current study, we demonstrate that Mbd2 plays a key role in RGC apoptosis that is caused by I/R injury. Mechanistically, Mbd2 can directly upregulate Mbd2-associated lncRNA 1 (Mbd2-AL1), which acts as a ceRNA, by directly binding to miRNA (miR)-188-3p and contributing in the downregulation of tumor necrosis factor (TNF) receptor-associated factor 3 (Traf3) expression during ischemic stress. Finally, our data reveal that in Mbd2-knockout (KO) mice, the I/R-induced RGC apoptosis is attenuated via a mechanism involving a targeted Mbd2-AL1/miR-188-3p/Traf3 axis. In this research, we determined the role of Mbd2 and its regulatory mechanism and further uncovered the pathology of RGC apoptosis in retinal ischemia.

RESULTS

The Expression of Mbd2 Is Induced by I/R in RGCs and Mice Retina

We first developed ischemia models, *in vitro* and *in vivo*, to detect the expression of Mbd2. Immunoblotting results indicated that Mbd2 was upregulated within the 2-h reperfusion and gradually reached a

Received 13 November 2019; accepted 3 January 2020;
https://doi.org/10.1016/j.omtn.2020.01.011.

Correspondence: Huiling Li, MD, Department of Ophthalmology, the Second Xiangya Hospital, Central South University, Changsha, 410011 Hunan, China.
E-mail: lihuiling@csu.edu.cn

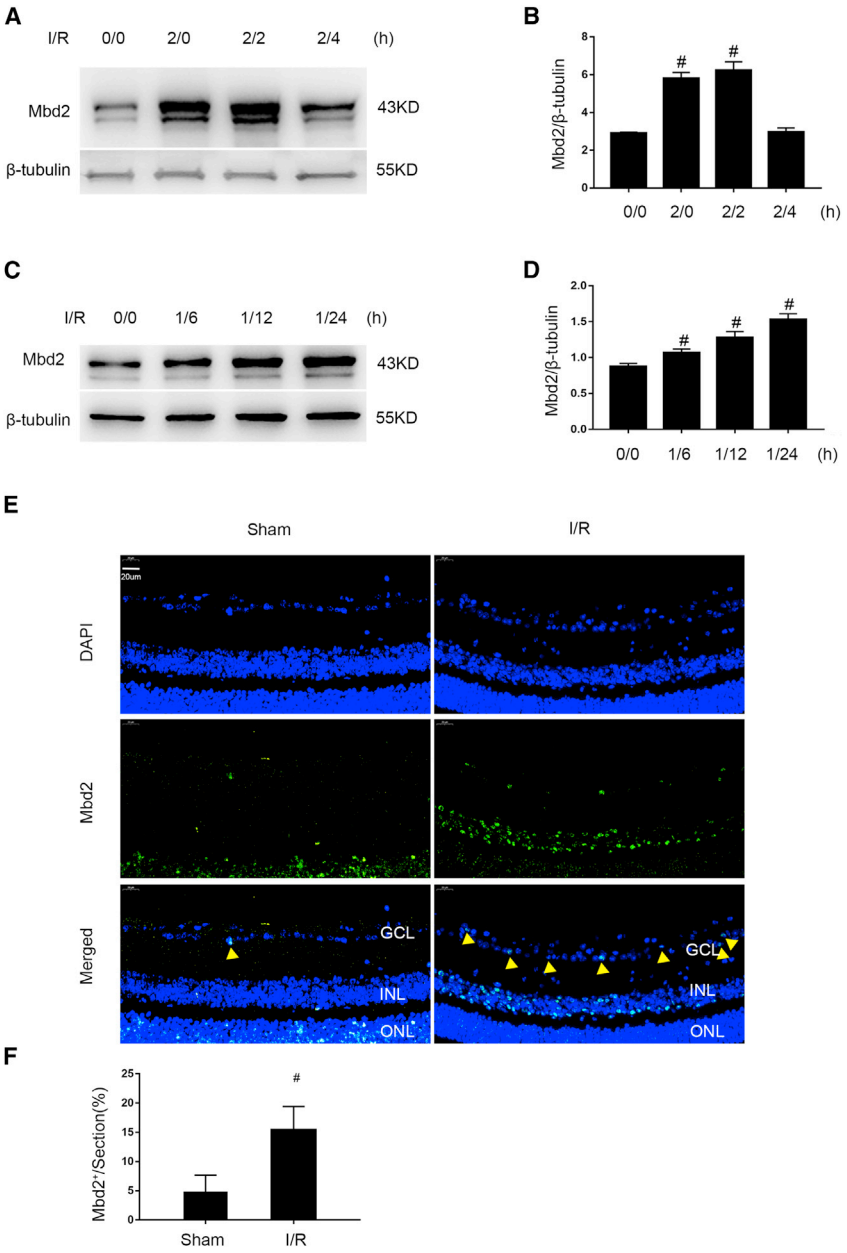

Figure 1. I/R Induced the Expression of Mbd2 in Mice RGCs and Retinas

(A and B) Cultured primary mouse RGCs were treated with or without Ca^{2+} (2 μM) and antimycin (10 μM) in HBSS (ATP and glucose depletion) at indicated time periods (ischemia/reperfusion for 0/0 h, 2/0 h, 2/2 h, and 2/4 h, respectively). Mbd2 levels were analyzed by western blotting. I/R induces an increase of Mbd2 levels in mice RGCs. The data are shown as mean ± SEM of five independent experiments. #$p < 0.05$ versus the 0/0 group. (C and D) The intraocular pressure was elevated to 120 mmHg for 1 h to induce a transient retinal ischemia and then exposed to reperfusion for 6 h, 12 h, and 24 h in C57BL/6 mice, respectively. The level of Mbd2 expression gradually increased in the retinas following ischemic reperfusion injury. Immunoblot signals were quantified by densitometry and normalized to the internal control β-tubulin. The data are shown as mean ± SEM of five independent experiments. #$p < 0.05$ versus the 0/0 group. (E and F) Immunofluorescent staining of retinal sections from 24-h reperfusion and after 1 h ischemia compared with control animals. The green signal represents the subcellular localization of Mbd2 in nucleus. The number of Mbd2-positive cells in the RGC layer was significantly higher than in the sham group (yellow arrowheads). The data are shown as mean ± SEM of five independent experiments. #$p < 0.05$ versus the sham group.

peak level at 2 h, and that was followed by a decline to base level at 4 h in primary RGCs (Figures 1A and 1B). Consistently, Mbd2 was also gradually upregulated 6 h after reperfusion and achieved a 24-h peak level in mice retina (Figures 1C and 1D). Immunofluorescent analysis further demonstrated that Mbd2 was expressed in the inner-neural retina after ischemic injury, especially in RGC nuclei (Figures 1E and 1F). Collectively, these results suggest that I/R injury can induce the expression of Mbd2 *in vitro* and *in vivo*.

Mbd2 Mediates RGC Apoptosis Caused by I/R Injury

To determine the potential role of Mbd2 in RGC apoptosis induced by ischemia injury, Mbd2 small interfering RNA (siRNA) or Mbd2 plasmid was transfected into RGCs. 2 h after reperfusion, the results of flow cytometry (FCM) analysis demonstrated that downregulation of Mbd2 by siRNA markedly attenuated ischemia-induced RGC apoptosis (Figures 2A and 2B). Consistently, immunoblotting analysis indicated that Mbd2 siRNA also suppressed the activation of caspase3 and the expression of Mbd2 (Figures 2C–2F). In contrast, these effects following I/R injury were enhanced by Mbd2 overexpression (Figures 2G–2L). These data indicate that Mbd2 mediates ischemia-induced RGC apoptosis *in vitro*.

lncRNA ENSMUST00000160470 (Mbd2-AL1) Induced by I/R Is Inhibited by Mbd2 siRNA

Although we have demonstrated that Mbd2 mediated I/R-induced RGC apoptosis, the mechanism of regulation remains unclear. We hypothesize that Mbd2 promoted RGC apoptosis via the regulation of lncRNA expression. A lncRNA chip was used to detect the changes of lncRNAs in scramble, ischemia, and Mbd2 siRNA with ischemia groups (Figure 3A). I/R induced the upregulation of 416 lncRNAs (>4-fold change) in the scramble-with-I/R versus scramble group (Table S1), whereas downregulated 315 genes in the Mbd2-siRNA group (Table S2). Interestingly, 13 of the 315 downregulated lncRNA promoter regions exhibited the CpG island with the highest upregulation fold changes (Figure 3B). Among them, ENSMUST00000160470 and ENSMUST00000123262 ranked first and second, respectively. Quantitative real-time PCR supported

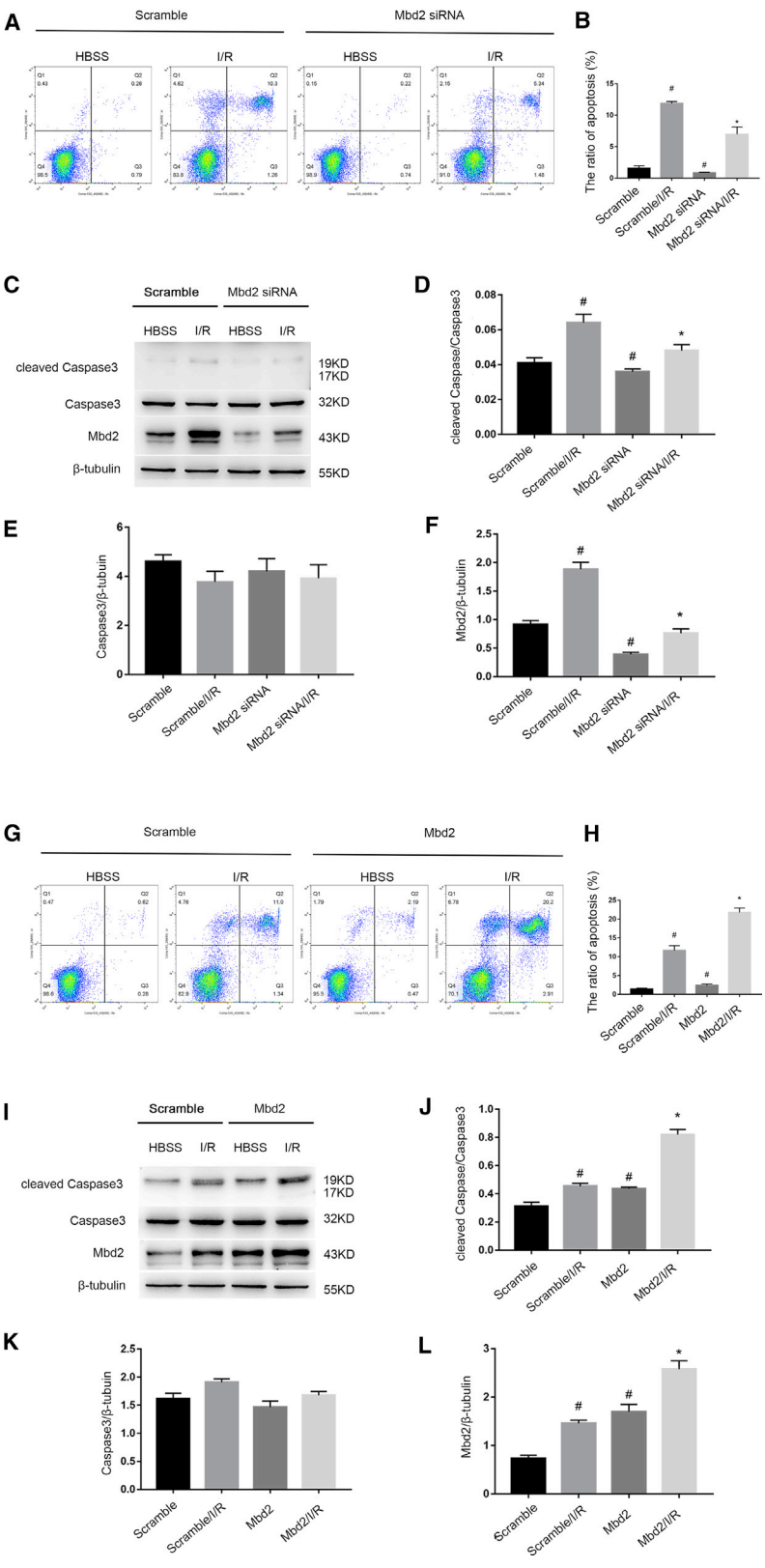

Figure 2. Mbd2 Can Mediate RGC Apoptosis Caused by I/R Injury

RGCs were transfected with 50 nM Mbd2 siRNA or 1 μg/mL Mbd2 plasmid or scramble for 24 h and then left treated or untreated with ischemic stress for 2 h, followed by reperfusion for 2 h to induce apoptosis. (A and B) Representative flow cytometric data and cell apoptosis analysis results from four experimental groups showed that the knockdown of Mbd2 expression led to a significantly lower RGC apoptosis after I/R injury. (C–F) Western blot showed that Mbd2 siRNA significantly suppressed the expression of Mbd2 and cleaved caspase3. (G and H) Representative flow cytometric data and cell apoptosis analysis results indicated that the overexpression of Mbd2 can aggravate RGC apoptosis upon I/R. (I–L) The level of Mbd2 and cleaved caspase3 was significantly increased when RGCs were transfected with Mbd2 plasmid. Data were expressed as mean ± SEM of five independent experiments. #$p < 0.05$ versus the scramble group; *$p < 0.05$ versus the scramble/I/R group.

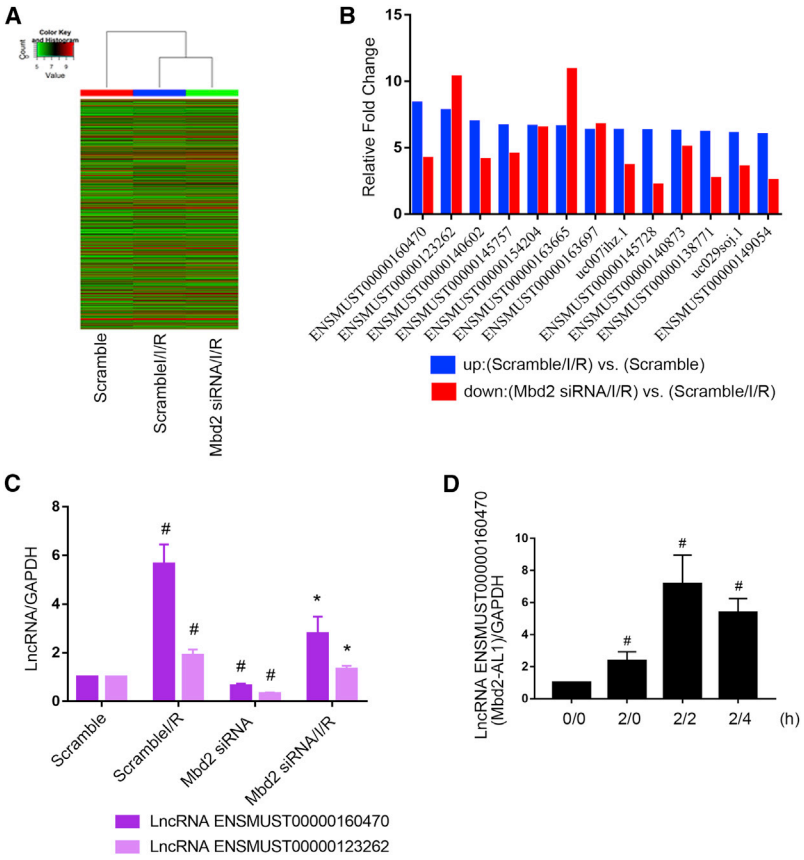

Figure 3. The Induction of lncRNA ENSMUST00000160470 (Mbd2-AL1) by I/R Is Inhibited by Mbd2 siRNA in RGCs

RGCs were transfected with 50 nM Mbd2 siRNA or scramble for 24 h and then left treated or untreated with ischemia for 2 h and reperfusion for another 2 h. (A) Representative heatmap of lncRNA microarray analysis. (B) The amount of each lncRNA from the scramble/I/R group divided by the amount of the scramble group to calculate the up-fold change and from the Mbd2 siRNA/I/R group divided by the scramble/I/R group getting the down-fold change. (C) Quantitative real-time PCR analysis of ENSMUST00000160470 and ENSMUST00000123262. The value of each lncRNA was normalized by glyceraldehyde 3-phosphate dehydrogenase (GAPDH), an internal control. Data were expressed as mean ± SEM of five independent experiments. #$p < 0.05$ versus the scramble group; *$p < 0.05$ versus the scramble/I/R group. (D) The levels of lncRNA ENSMUST00000160470 (Mbd2-AL1) induced by I/R treatment at indicated time points (0 h, 2 h, and 4 h). Data were expressed as mean ± SEM of five independent experiments. #$p < 0.05$ versus the 0/0 group.

the findings obtained from the lncRNA chip experiment (Figure 3C) and further indicated that reperfusion induced the expression of ENSMUST00000160470 at indicated time points and reached the peak at 2 h after reperfusion (Figure 3D). The data indicate that lncRNA ENSMUST00000160470 (Mbd2-AL1) may be a target of Mbd2.

Mbd2 Suppresses Promoter Methylation of Mbd2-AL1 and Activates Its Demethylation

Although Mbd2 mediated the expression of Mbd2-AL1, the mechanism of regulation remains unclear. To investigate this, we performed a CpG island prediction analysis and primers design *in silico* (MethPrimer 2.0 software) (Figure 4A). Among five pair primers, only mBS4 was identified as a potential Mbd2 binding site in the Mbd2-AL1 promoter region and assessed by the chromatin immunoprecipitation (ChIP) assay (Figure 4B). The methylated cytosine and guanine (CG) DNA of the Mbd2-AL1 promoter was cloned into the pCpGfree-basic-Lucia (pCpGl) plasmid and cotransfected with Mbd2 or mutational Mbd2 (mtMbd2; depletion of DNA methylation domain) plasmids. The transcription activity was enhanced by Mbd2 overexpression but not mtMbd2 (Figure 4C). Furthermore, methylation level analysis indicated that methylated pCpGl of Mbd2-AL1 was inhibited by the endogenous Mbd2, and the effect was reinforced by ectopic Mbd2 expression (Figure 4D). Thus, Mbd2 siRNA suppressed the expression of Mbd2-AL1, and this could be reversed by overexpressing Mbd2 (Figures 4E and 4F). Taken together, Mbd2 binds to the promoter region of Mbd2-AL1 and is associated with its demethylation.

Mbd2-AL1 Mediates I/R-Induced RGCs Apoptosis

To further verify the role of Mbd2-AL1 in the RGC apoptosis induced by I/R, Mbd2-AL1 siRNA or Mbd2-AL1 plasmids were transfected into RGCs and were subjected to ischemic treatment. 2 h after reperfusion, the FCM analysis indicated that RGC apoptosis was attenuated by Mbd2-AL1 siRNA (Figures 5A and 5B). By contrast, the effect was enhanced by Mbd2-AL1 overexpression (Figures 5G and 5H). The quantitative real-time PCR results indicated that the expression of Mbd2-AL1, induced by I/R, was suppressed by Mbd2-AL1 siRNA (Figure 5C); however, this effect was enhanced with the Mbd2-AL1 plasmid (Figure 5I). Consistently, the immunoblotting results also demonstrated an activation of caspase3, and that was inhibited by Mbd2-AL1 siRNA (Figures 5D–5F). However, the effect was increased with the Mbd2-AL1 plasmid (Figures 5J–5L). Collectively, the data suggest that Mbd2-AL1 is an apoptosis inducer during ischemia injury.

miR-188-3p Is a Direct Target of lncRNA Mbd2-AL1

A previous study suggested that lncRNAs act as a "sponge" through their association with miRNAs and to regulate target gene expression.[20] We predicted that Mbd2-AL1 exhibited complementary sequences to miR-188-3p using the *in silico* RegRNA software. The sequences of complementary and mutated Mbd2-AL1 (Mbd2-AL1 wild type [WT] and Mbd2-AL1 mutant [MUT], respectively) were cloned into a luciferase reporter plasmid, respectively (Figures 6A and 6B). The results indicated that the miR-188-3p mimic suppressed the luciferase activity of

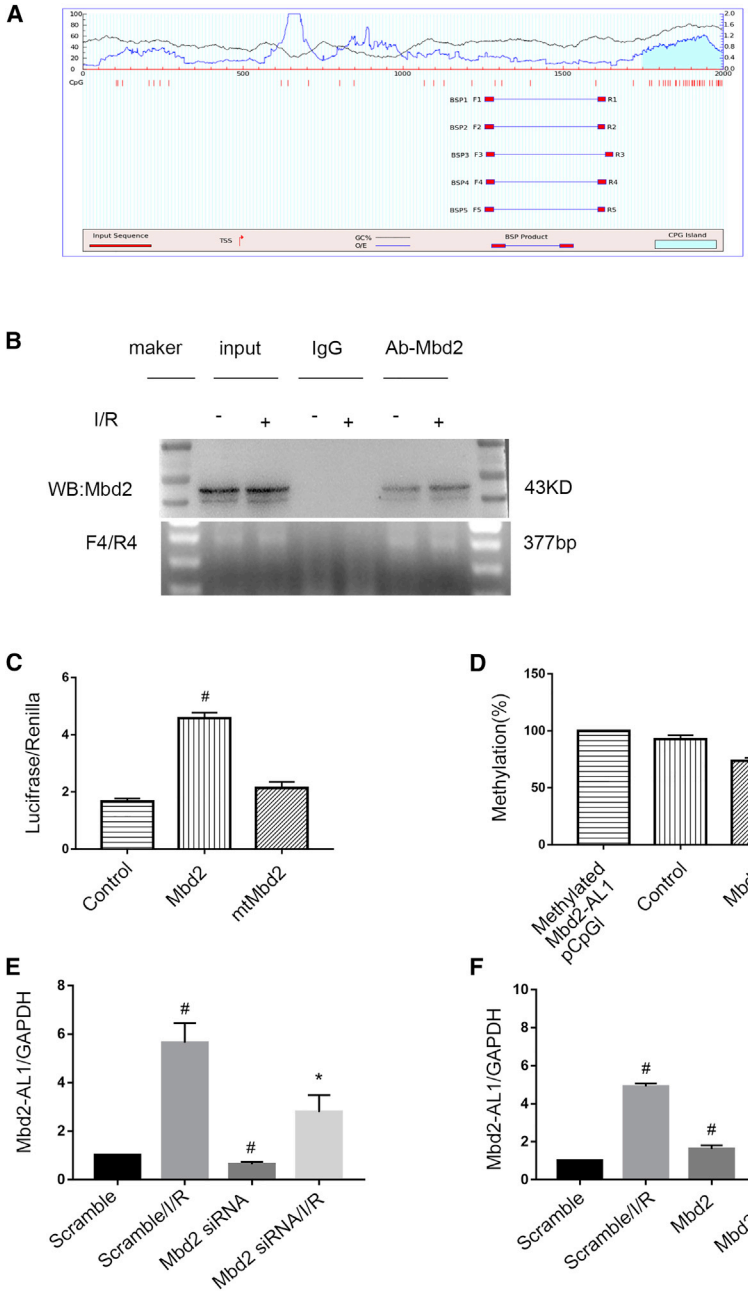

Figure 4. Mbd2 Suppresses the Methylation of the lncRNA Mbd2-AL1 Promoter and Activates Its Demethylation

(A) The CpG island of the Mbd2-AL1 promoter was predicted, and five primer pairs were designed by the software MethPrimer 2.0. (B) ChIP assays were performed with chromatin materials, isolated from RGCs, treated with I/R, and precipitated with Mbd2, IgG, or without antibody (input) and used as a template for PCR detection of potential Mbd2 binding site 4 (mBS4). (C) Relative luciferase activity in RGCs. Cotransfection of Mbd2 plasmid, mtMbd2 plasmid, or control with the pCpGfree-basic luciferase reporter plasmid containing the promoter region of Mbd2-AL1. The data were expressed as mean ± SEM of five independent experiments. #$p < 0.05$ versus mtMbd2. (D) The percentage of CpG-DNA methylation of the Mbd2-AL1 promoter. Cotransfection of the Mbd2 plasmid or control with the pCpGfree-basic luciferase reporter plasmid containing the methylated promoter region of Mbd2-AL1. The data were expressed as mean ± SEM of five independent experiments. #$p < 0.05$ versus the control group. (E and F) Quantitative real-time PCR of the expression of lncRNA Mbd2-AL1 in RGCs. (E) Mbd2 siRNA suppressed the expression of Mbd2-AL1. (F) The expression of Mbd2-AL1 in RGCs was upregulaed after transfection of exogenous Mbd2 plasmid. The data were expressed as mean ± SEM of five independent experiments. #$p < 0.05$ versus the scramble group; *$p < 0.05$ versus the scramble/I/R group.

Mbd2-AL1 WT, instead of the Mbd2-AL1 MUT (Figure 6B). Furthermore, the expression of miR-188-3p was enhanced by Mbd2-AL1 siRNA. In contrast, the effect was reversed by Mbd2-AL1 overexpression (Figures 6C and 6D). Besides, the fluorescence *in situ* hybridization (FISH) array experiment indicated that Mbd2-AL1 and miR-188-3p colocalized in RGC cytoplasm of the control group and that these effects were enhanced by I/R treatment (Figure 6E). These findings suggest that Mbd2-AL1 has a sponging effect on miR-188-3p in RGCs.

I/R-Induced RGC Apoptosis Is Suppressed by the Overexpression of miR-188-3p

A previous study has reported that miR-188-3p inhibits apoptosis of spermatogenic cells.[21] It is still unclear whether miR-188-3p has the same function in I/R-induced apoptosis of RGCs. Two hours after reperfusion, FCM analysis indicated that the miR-188-3p mimic markedly suppressed I/R-induced RGC apoptosis (Figures 7A and 7B). Quantitative real-time PCR analysis indicated that the expression of miR-188-3p was suppressed by I/R treatment, which was reversed by the miR-188-3p mimic (Figure 7C). Finally, the miR-188-3p mimic significantly suppressed the activation of caspase3 (Figures 7D–7F). These results reveal that miR-188-3p suppresses I/R-induced RGC apoptosis.

The Apoptosis Inducer Traf3 Is a Target Gene of miR-188-3p

One study reported that the TNF receptor-associated factor 3 (Traf3) protein is an apoptosis inducer in malignant human urothelial cells.[22] The prediction result indicates that Traf3 is a target gene of miR-188-3p using the miRbase analysis website (Figure 8A). The luciferase activity of Traf3-WT, instead of Traf3-MUT, was suppressed by the miR-188-3p mimic (Figure 8B).

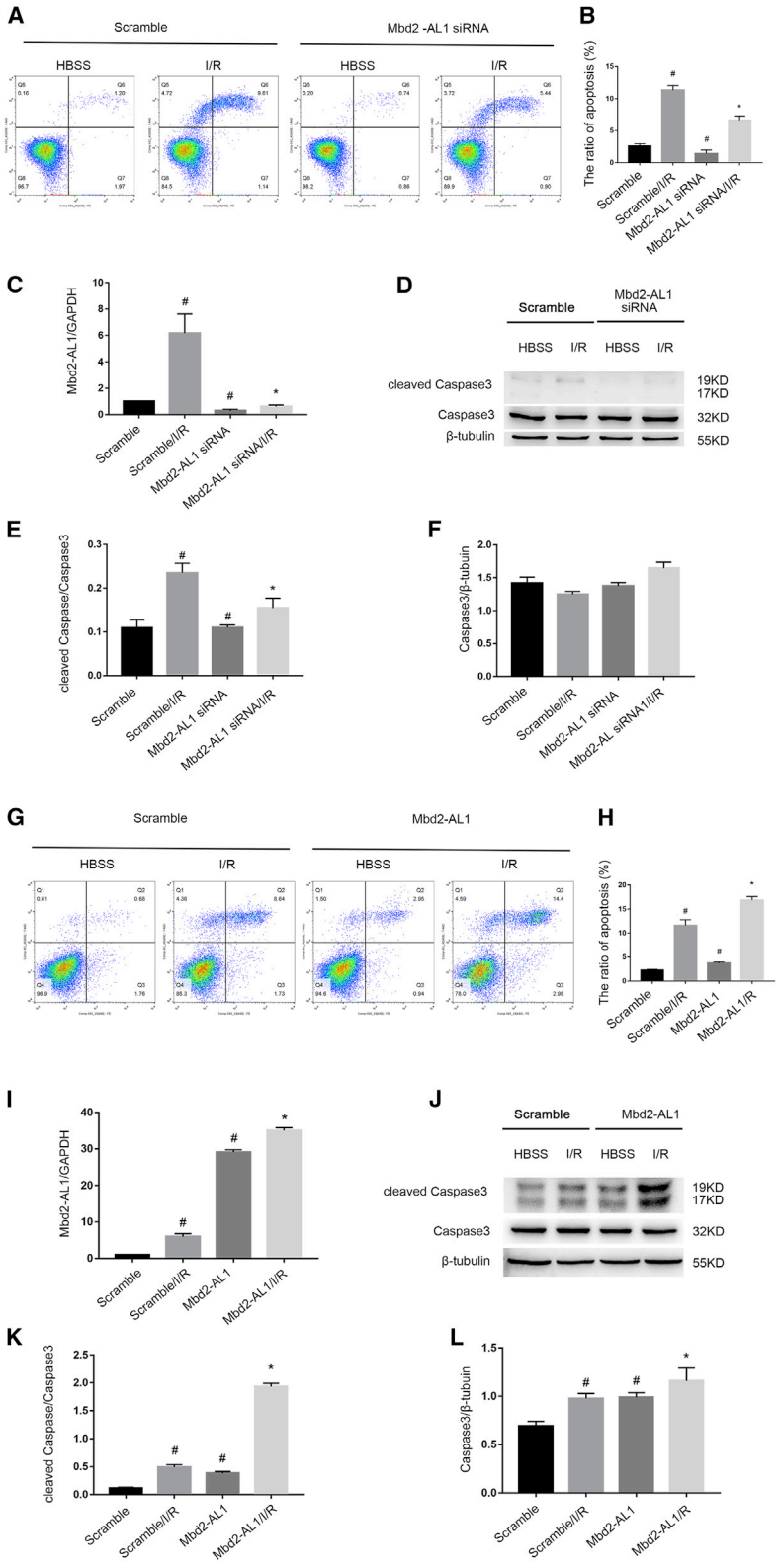

Figure 5. lncRNA Mbd2-AL1 Mediates RGC Apoptosis upon I/R Injury

RGCs were transfected with 50 nM Mbd2-AL1 siRNA or 1 μg/mL Mbd2-AL1 plasmid or scramble, 24 h before I/R and following I/R for 2/2 h. (A and B) Representative flow cytometry data and statistical analysis results of cell apoptosis from four experimental groups showing that the deletion of Mbd2-AL1 attenuated I/R-induced RGC apoptosis. (C) The levels of Mbd2-AL1, with or without I/R treatment, were analyzed by quantitative real-time PCR. The level of Mbd2-AL1 was increased after I/R interference. Mbd2-AL1 siRNA suppressed the expression of Mbd2-AL1 in both scramble and I/R group. (D–F) Western blot results showing the expression of cleaved caspase3 and caspase3 with statistical data analysis. β-Tubulin was used as internal control. Mbd2-AL1 siRNA could suppress the expression of cleaved caspase3 induced by I/R injury. (G and H) Representative flow cytometric data and statistical analysis results of cell apoptosis from four experimental groups showed that the overexpression of Mbd2-AL1 aggravated I/R-induced apoptosis. (I) Quantitative real-time PCR showing the levels of Mbd2-AL1, with or without I/R treatment. The level of Mbd2-AL1 was increased after I/R injury. Transfection of exogenous Mbd2-AL1 plasmid significantly increased the expression level of Mbd2-AL1 in both scramble and I/R group. (J–L) Western blot showing the expression of cleaved caspase3 and caspase3 with statistical data analysis. Transfection of exogenous Mbd2-AL1 plasmid increased the expression of cleaved caspase3 in both scramble and I/R group. β-Tubulin was used as internal control. The data were expressed as mean ± SEM of five independent experiments. #$p < 0.05$ versus the scramble group; *$p < 0.05$ versus the scramble/I/R group.

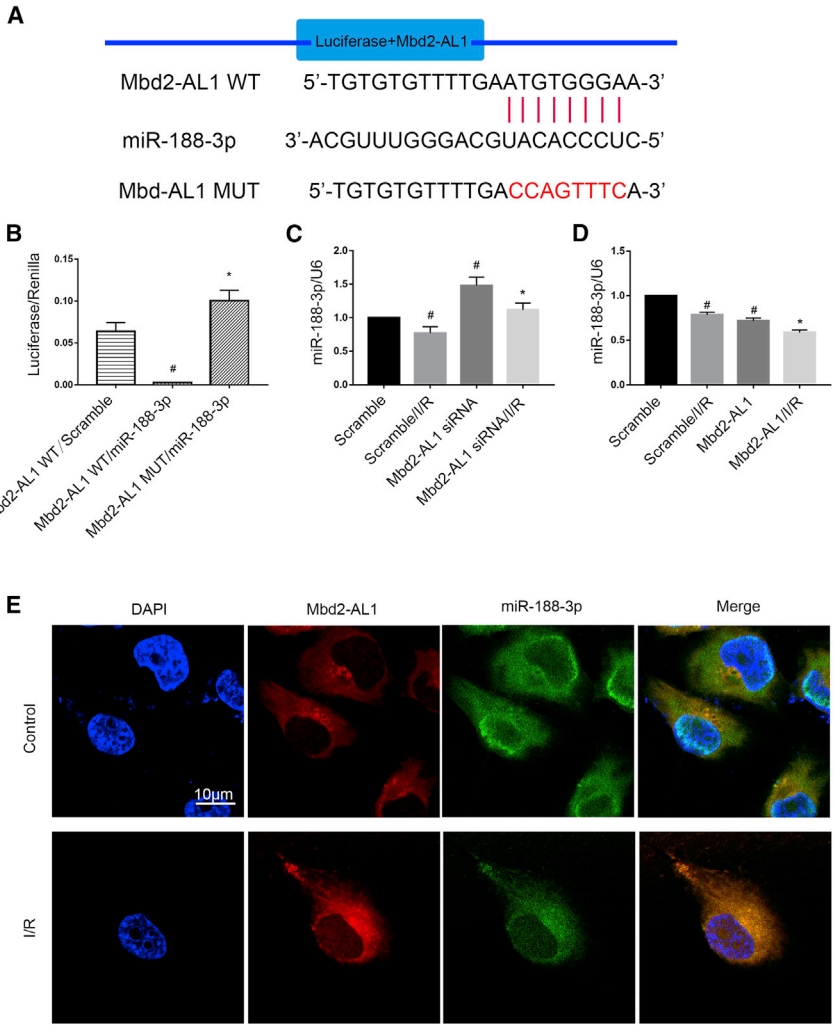

Figure 6. miR-188-3p Is a Direct Target of lncRNA Mbd2-AL1

(A) The sequence-alignment analysis revealed that Mbd2-AL1 RNA contains a complementary site to miR-188-3p. (B) Luciferase activity, assessed 48 h after cotransfection of lncRNA Mbd2-AL1 WT or Mbd2-AL1 MUT plasmid with miR-188-3p mimic or scramble. (C) Knockdown of lncRNA Mbd2-AL1 increases the expression level of miR-188-3p. RGCs were transfected with 50 nM Mbd2-AL1 siRNA and then left treated or untreated with ischemic stress for 2 h and reperfusion for 2 h. (D) Overexpression of Mbd2-AL1 induces the reduction of miR-188-3p expression level. RGCs were transfected with 50 nM Mbd2-AL1 plasmid and then left treated or untreated, as described in (C). miR-188-3p expression levels were analyzed by quantitative real-time PCR in (C) and (D). (E) The intracellular colocalization of Mbd2-AL1 and miR-188-3p in RGCs, with or without I/R treatment. Data were expressed as mean ± SEM of five independent experiments. #$p < 0.05$ versus the Mbd2-AL1/scramble or scramble group, *$p < 0.05$ versus Mbd2-AL1 WT/miR-188-3p mimic or the scramble/I/R group.

Furthermore, miR-188-3p notably abrogated Traf3 basal and I/R-induced mRNA and protein expression (Figures 8C–8E). In addition, Traf3 was induced by I/R at the indicated time point (Figures 8F and 8G). Finally, the suppression of Traf3 markedly attenuated I/R-induced RGC apoptosis and the activation of caspase3 (Figures 8H–8M). These data reveal that Traf3, a direct target of miR-188-3p, mediates I/R-induced RGC apoptosis.

Mbd2-AL1 Mediates I/R-Induced RGC Apoptosis by Targeting miR-188-3p

We further explored the role of miR-188-3p in Mbd2-AL1-mediated, I/R-induced RGC apoptosis. To this end, we tested whether the knockdown of miR-188-3p reverses the apoptotic effect of Mbd2-AL1 siRNA. FCM analysis showed that Mbd2-AL1 siRNA mitigated RGC apoptosis; in contrast, the effect was reversed by the miR-188-3p inhibitor (Figures 9A and 9B). By quantitative real-time PCR, the levels of Mbd2-AL1 and miR-188-3p were detected following transfection (Figures 9C and 9D). In the meantime, the levels of Traf3 and cleaved caspase3 that were induced by I/R were suppressed by Mbd2-AL1 siRNA but abrogated by the miR-188-3p inhibitor (Figures 9E–9H). Collectively, these data demonstrate that Mbd2-AL1 mediates I/R-induced RGC apoptosis by targeting miR-188-3p.

Deletion of Mbd2 Ameliorates RGC Apoptosis and Preserves Retinal Function Following I/R Injury

To further determine the effects of Mbd2 in ischemia-induced RGC apoptosis *in vivo*, we quantified RGCs by specific Tuj1 (neuronal class III β-tubulin) staining and terminal-deoxy-transferase-mediated 2′-deoxyuridine, 5′-triphosphate (dUTP) nick end-labeling (TUNEL) staining and evaluated retinal function in Mbd2 knockout mice following I/R injury. Compared with the Mbd2-WT mice at 7 days following I/R stress (1,100 ± 240 RGC/mm^2), mice lacking Mbd2 showed significantly higher levels of RGC survival (2,400 ± 140 RGC/mm^2); however, RGC survival remained lower than those in sham controls (3,610 ± 220 RGC/mm^2) (Figures 10A and 10B). 24 h after reperfusion, the TUNEL-positive staining was significantly decreased in Mbd2-KO mice retinas compared with Mbd2-WT mice retinas (Figures 10C and 10D). Along with our morphological results, we also performed a scotopic electroretinogram (ERG) to evaluate changes in retinal function of Mbd2-WT and Mbd2-KO mice, 2 and 7 days after reperfusion. We noticed significantly decreased b-wave amplitudes in all mice (Figures 10E and 10F). However, Mbd2-KO eyes displayed statistically significant recoveries at these two time points when compared with WT mice eyes. In summary, these results confirm that the deletion of Mbd2 ameliorates RGC apoptosis and delays loss of visual function following I/R injury *in vivo*.

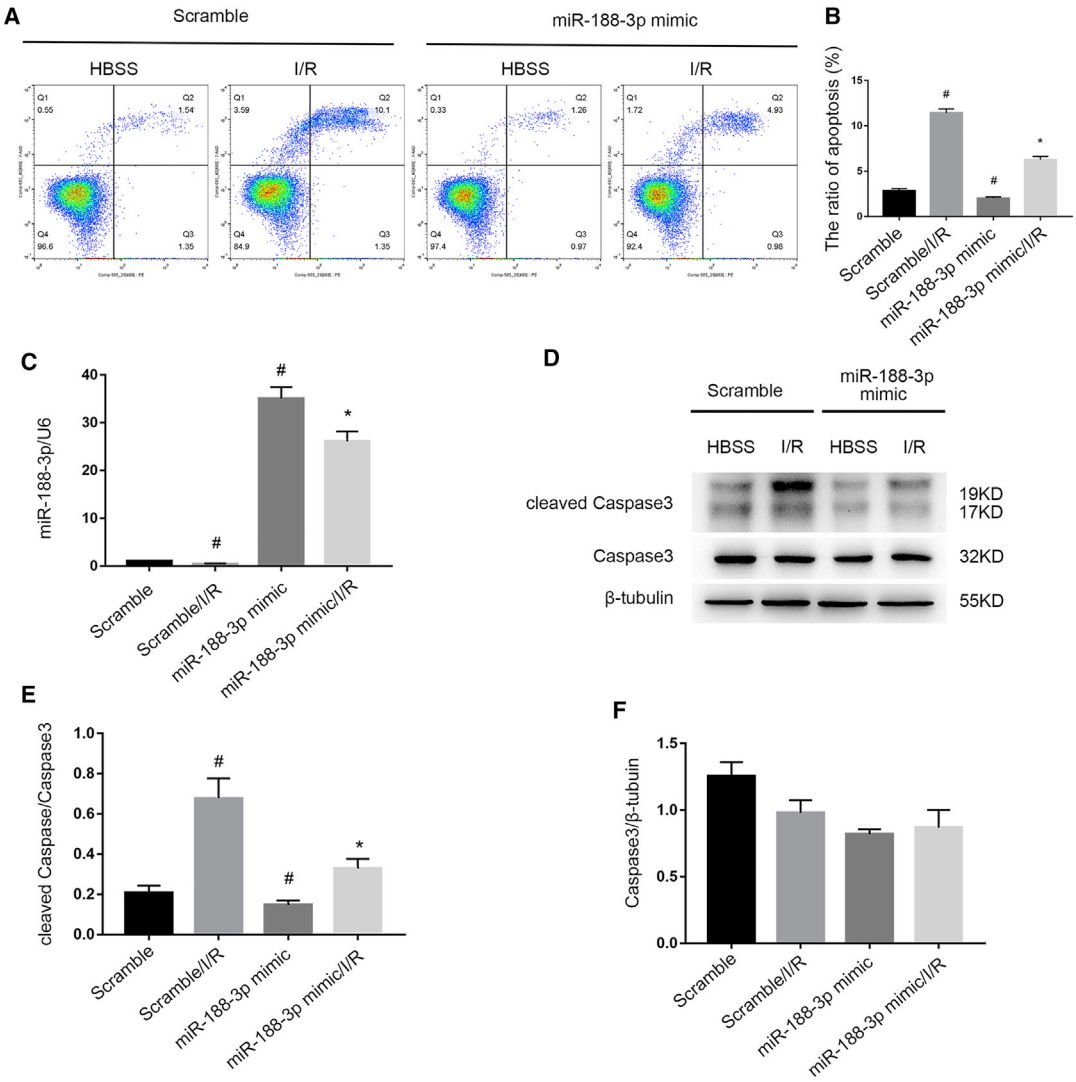

Figure 7. The I/R-Induced RGC Apoptosis Is Suppressed by the Overexpression of miR-188-3p

RGCs were transfected with 50 nM miR-188-3p mimic or scramble, 24 h before I/R of 2/2 h. (A and B) Overexpression of miR-188-3p prevents RGC apoptosis that was induced by I/R. Apoptosis was analyzed by flow cytometry. (C) The expression level of miR-188-3p during I/R treatment or miR-188-3p mimic transfection. Quantitative real-time PCR is used to detect the miR-188-3p level. The value of the microRNA was normalized by the level of U6, an internal control. (D–F) The expression of cleaved caspase3 and caspase3 were analyzed by western blotting. The data were expressed as mean ± SEM of five independent experiments. #$p < 0.05$ versus the scramble group; *$p < 0.05$ versus scramble/I/R group.

I/R-Induced RGC Apoptosis Was Attenuated via the lncRNA Mbd2-AL1/miR-188-3P/Traf3 Axis in Mbd2-KO Mice

Since Mbd2 silencing protects I/R-induced RGC apoptosis in mice retina, we aimed to confirm the molecular mechanism *in vivo*. Quantitative real-time PCR analysis showed an upregulation of lncRNA Mbd2-AL1 in retina of the I/R model, which was decreased when Mbd2 was knocked out (Figure 11A). As expected, miR-188-3p was decreased by I/R and recovered in Mbd2-KO mice (Figure 11B). Moreover, immunoblotting showed that the expression of Mbd2, Traf3, and cleaved caspase3 was elevated in ischemic retina; however, Mbd2 deletion can significantly suppress the expression of apoptosis-related genes (Figures 11C and 11D). The data demonstrate that Mbd2 mediated I/R-induced RGC apoptosis in mice retina via the lncRNA Mbd2-AL1/miR-188-3P/Traf3 axis (Figure 12).

DISCUSSION

Previous studies have demonstrated that DNA methylation was involved in retinal cell death.[23,24] In the current study, we demonstrate, for the first time, that the DNA methylation reader Mbd2 mediates I/R-induced RGC apoptosis in primary RGCs. Mechanistically, Mbd2 upregulated the expression of lncRNA Mbd2-AL1 via the

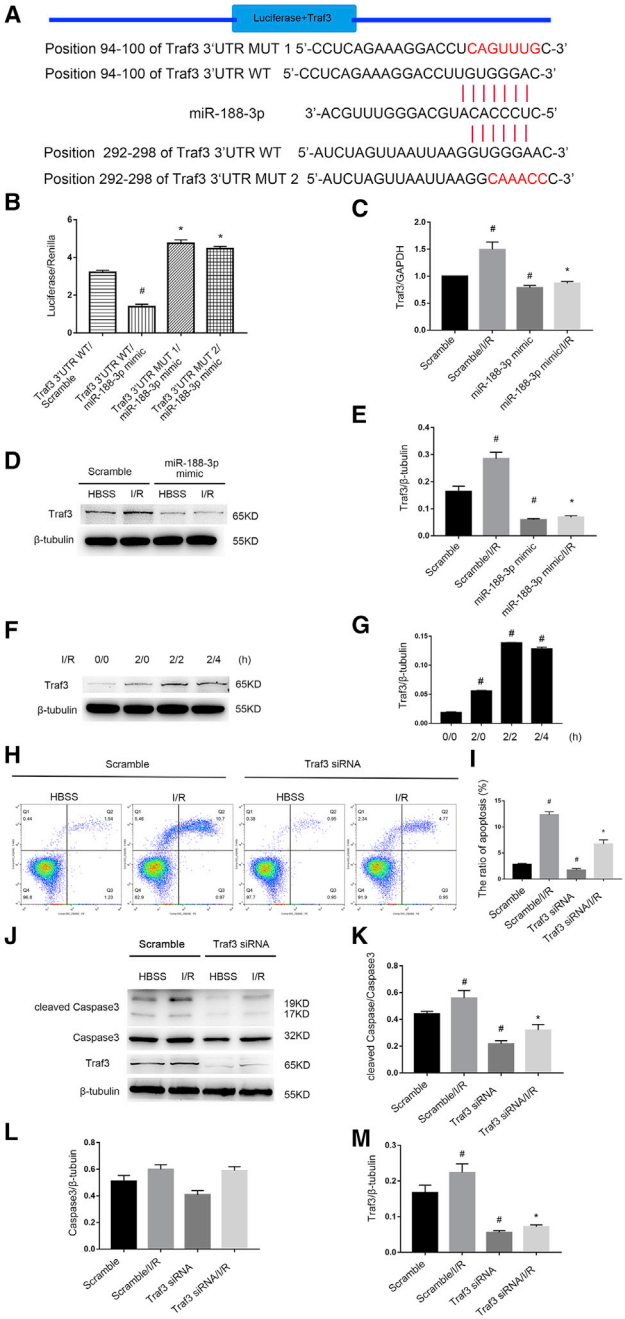

Figure 8. The Apoptotic Inducer Traf3 Is a Target Gene of miR-188-3p

RGCs were transfected with 50 nM of miR-188-3p mimic, Traf3 siRNA, or scramble, 24 h before I/R of 2/2 h. (A) Putative miR-188-3p complementary binding sites in the 3′ UTR region of mouse Traf3. (B) Detection of luciferase activity, 48 h after transfection of miR-188-3p mimic or scramble and the luciferase constructs of Traf3 3′ UTR WT or Traf3 3′ UTR MUT1 (position 94–100 of Traf3 3′ UTR) or Traf3 3′ UTR MUT2 (position 292–298 of Traf3 3′ UTR). The data were expressed as mean ± SEM of five independent experiments. #p < 0.05 versus Traf3 3′ UTR WT/ scramble; *p < 0.05 versus Traf3 3′ UTR WT with miR-188-3p mimic. (C–E) miR-188-3p suppresses the expression of Traf3. Traf3 levels of expression were analyzed by quantitative real-time PCR in (C) and by western blot in (D) and (E). The data were expressed as mean ± SEM of five independent experiments. #p < 0.05 versus the scramble group; *p < 0.05 versus the scramble/I/R group. (F and G) The levels of Traf3 were induced by I/R treatment at indicated time points, which were analyzed by western blotting. The data were expressed as mean ± SEM of five independent experiments. #p < 0.05 versus the 0/0 grouop. (H and I) The knockdown of Traf3 expression by Traf3 siRNA attenuates apoptosis upon I/R. Cell apoptosis analysis by flow cytometry in each group. (J–M) Western blot showing that the knockdown of Traf3 significantly suppresses the expression of Traf3 and cleaved caspase3. The data were expressed as mean ± SEM of five independent experiments. #p < 0.05 versus the scramble group; *p < 0.05 versus the scramble/I/R group.

demethylation of its promoter, and MBD2-AL1 acted as a ceRNA, preventing miR-188-3p-induced downregulation of Traf3. Finally, Mbd2-KO mice had significantly attenuated I/R-induced apoptosis in retinal cells and visual function decline. Collectively, Mbd2 mediated I/R-induced RGC apoptosis via the Mbd2-AL1/miR-188-3p/Traf3 axis.

A previous study demonstrated that Mbd2 mediated ischemic injury in mice hindlimb.[12] A recent study revealed that Mbd2 was induced and promoted the upregulation of the glucocorticoid receptor in the hippocampus of maternal nurturing in mice.[25] So far, the role of Mbd2 in RGCs remains unclear. In the present study, we found that Mbd2 was localized in RGC nuclei and induced by I/R injury *in vitro* and *in vivo*. Furthermore, I/R-induced RGC apoptosis was attenuated by Mbd2 siRNA and enhanced by its overexpression. Finally, Mbd2-KO mice had a markedly decreased I/R-induced RGC apoptosis and improved visual functions. Thus, our data suggest that Mbd2 mediates RGC apoptosis following I/R injury.

In this study, we report for the first time that Mbd2 could regulate the expression of lncRNA to mediate RGC apoptosis following I/R injury. A recent study has reported that Mbd2 upregulates miR-301a-5p to mediate renal cell apoptosis during vancomycin treatment.[10] Although many studies reported that lncRNAs were involved in the progression of retinal diseases,[26–28] it is still unclear whether Mbd2 regulates the expression of lncRNAs. Here, we found that lncRNA Mbd2-AL1 was a direct target of Mbd2, as suggested by our results. First, the results of microarray analysis and quantitative real-time PCR indicated that Mbd2 siRNA notably suppressed the I/R-induced expression of lncRNA Mbd2-AL1; however, this effect was reversed by Mbd2 overexpression. Second, we found that Mbd2 upregulated the expression of Mbd2-AL1 via the demethylation of the promoter of Mbd2-AL1. Finally, Mbd2-KO mice had attenuated I/R-induced expression of lncRNA Mbd2-AL1. Collectively, these data show that Mbd2 directly regulates the expression of lncRNA Mbd2-AL1.

Recent studies reported that lncRNAs GAS5 and Sox2OT promoted the apoptosis of RGCs,[29,30] whereas lncRNA MALAT1 suppressed this effect.[31] Our data demonstrated that lncRNA Mbd2-AL1 mediated I/R-induced RGC apoptosis. As we know, lncRNA acted as a ceRNA to sponge miRNA.[32–34] For example, lncRNA antisense noncoding RNA in the INK4 locus (ANRIL) serves as a competing endogenous RNA to sponge miR-99a and promote apoptosis in retinoblastoma Y79

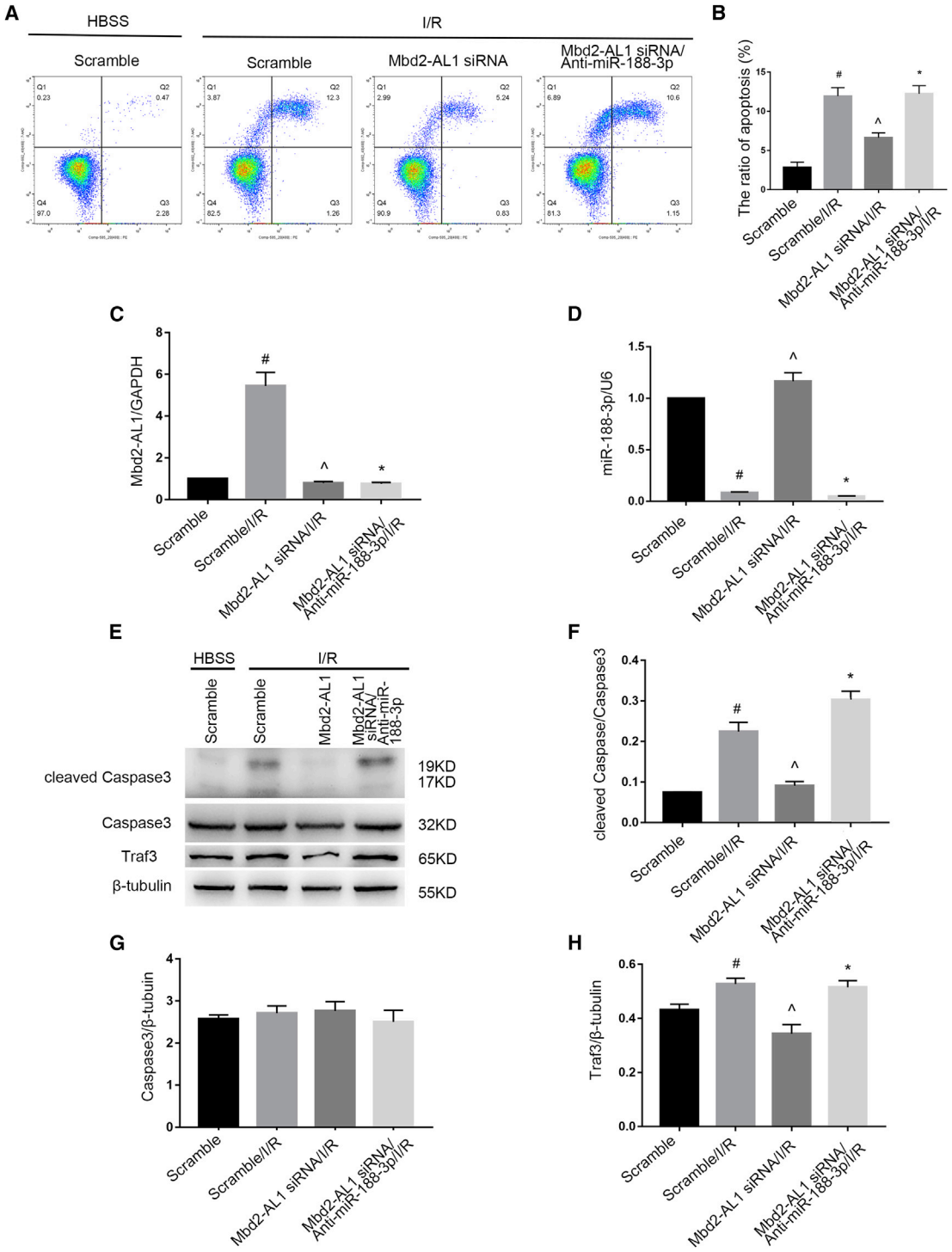

Figure 9. Mbd2-AL1 Mediates I/R-Induced RGC Apoptosis by Targeting miR-188-3p

RGCs were transfected with 50 nM Mbd2-AL1 siRNA or cotransfected with Mbd2-AL1 siRNA and miR-188-3p inhibitor, 24 h before I/R of 2/2. (A and B) The deletion of Mbd2-AL1 attenuates the apoptosis induced by I/R injury, and this effect was reversed by miR-188-3p knockdown. Apoptosis is analyzed by flow cytometry. (C and D) The levels of lncRNA Mbd2-AL1 and miR-188-3p were analyzed by quantitative real-time PCR. (E–H) The expression levels of cleaved caspase3, caspase3, and Traf3 were analyzed by western blotting. The data were expressed as mean ± SEM of five independent experiments. #$p < 0.05$ versus the scramble group; ^$p < 0.05$ versus the scramble/I/R; *$p < 0.05$ versus Mbd2-AL1 siRNA /I/R group.

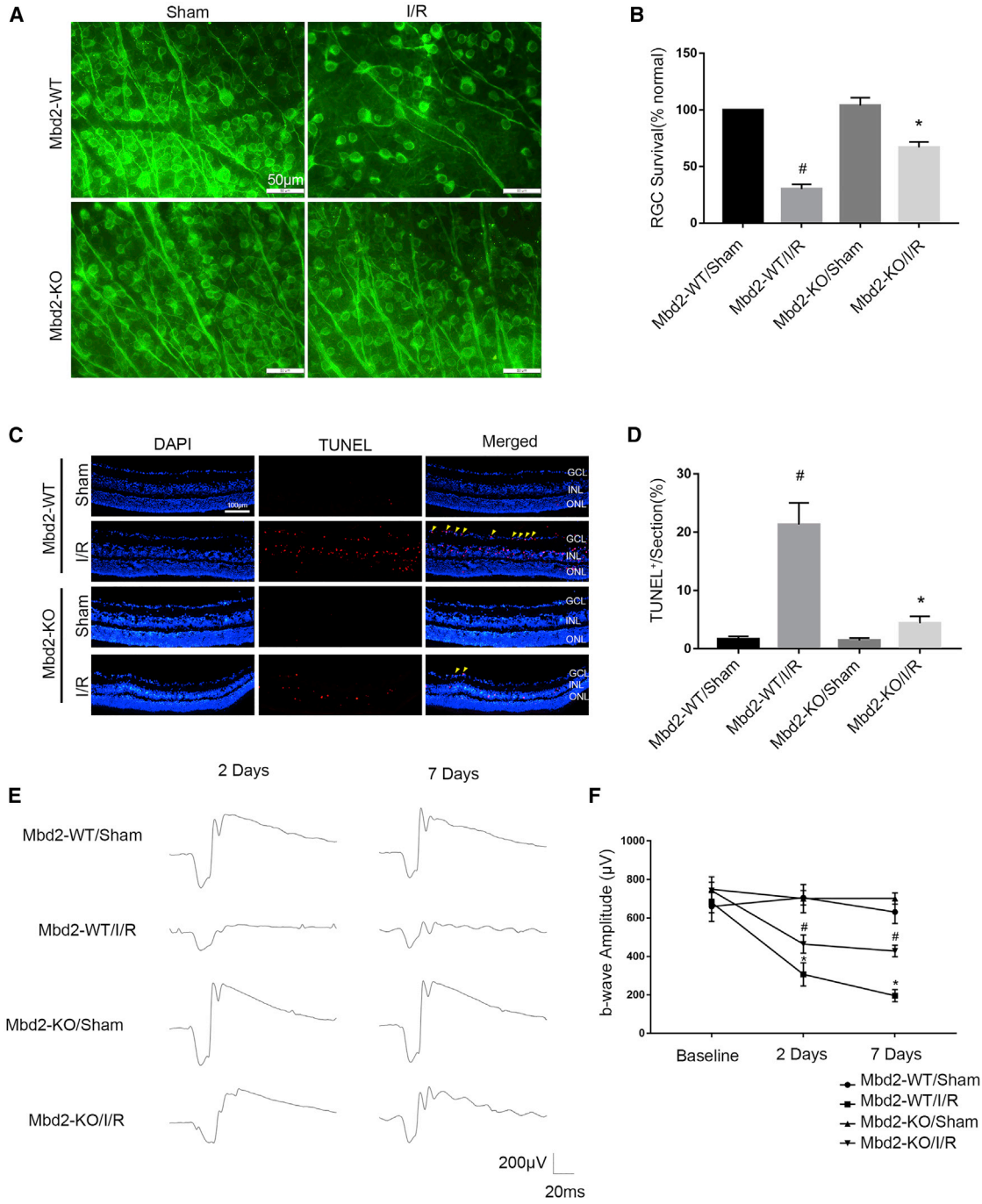

Figure 10. Knockout of Mbd2 Promotes RGC Survival in I/R injury

The intraocular pressure (IOP) of homozygous mice deficient in Mbd2 and wild-type littermates was elevated to 120 mmHg for 1 h, and the retinas were then dissected at indicated time points. (A and B) Effect of Mbd2 deletion on RGC survival *in vivo*. Representative images of retinal flat-mount immunostaining for Tuj1 to visualize surviving ganglion cells in mice at 7 days after induction of I/R or the sham group, with or without deletion of Mbd2. Original scale bars, 50 μm. Mean count of RGCs normalized to the Mbd2-WT/sham group. (C and D) Representative sections of TUNEL-positive cells in retina at 24 h after induction of I/R or the sham group, with or without deletion of Mbd2. Original scale bar, 100 μm. Mean number of TUNEL-positive RGCs normalized to total nuclei in the ganglion cell layer. Four central retina slices were analyzed per animal. (E and F) Representative scotopic ERG traces in Mbd2-WT and Mbd2-KO mice, with or without I/R, at an intensity of 3.0 cds/m^2 at 2 and 7 days postretinal ischemia. Comparison and statistical analysis of b-wave amplitudes among four groups at 3.0 cds/m^2 scotopic ERG. The data were expressed as mean ± SEM of five independent experiments. #$p < 0.05$ versus the Mbd2-WT/sham group; *$p < 0.05$ versus the Mbd2-WT/I/R group.

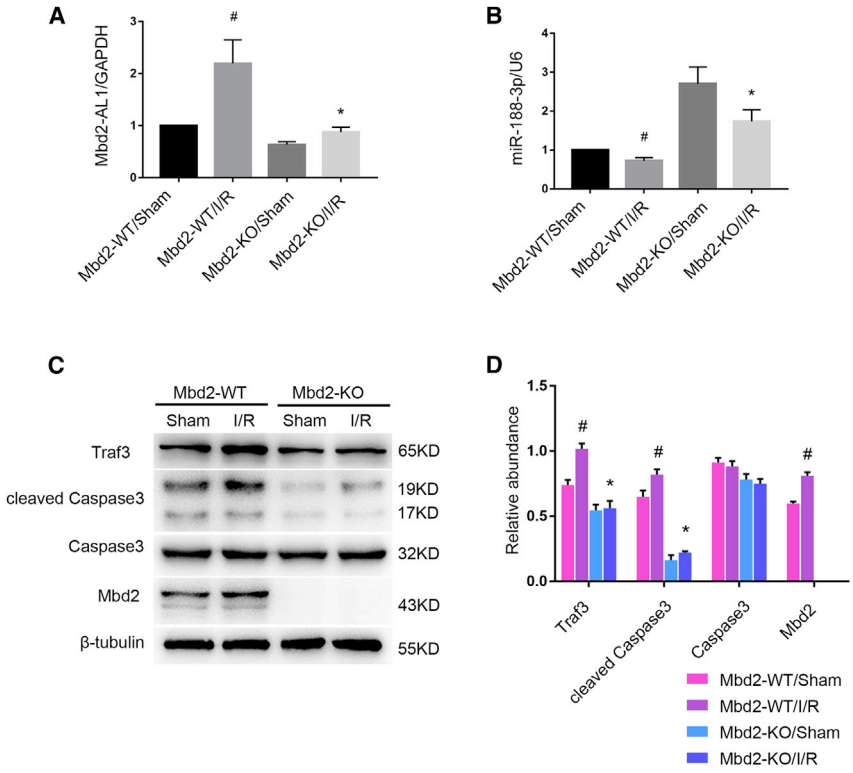

Figure 11. The Mbd2-KO Mice Attenuated I/R-Induced RGC Apoptosis via the lncRNA Mbd2-AL1/miR-188-3P/Traf3 Axis

The IOP of homozygous mice deficient in Mbd2 and wild-type littermates was elevated to 120 mmHg for 1 h, and the retinas were dissected 24 h later. (A and B) Quantitative real-time PCR analysis of the levels of lncRNA Mbd2-AL1 and miR-188-3p in retinas of four groups. (C and D) Western blot with statistical analysis showing the levels of Traf3, cleaved caspase3, and Mbd2 in 4 different groups. The data were expressed as mean ± SEM of five independent experiments. #$p < 0.05$ versus Mbd2-WT/sham group; *$p < 0.05$ versus Mbd2-WT/I/R group.

cells.[35] Hence, we predicted that miR-188-3p was a target gene of lncRNA Mbd2-AL1. Several experiments were performed to demonstrate this hypothesis. First, following I/R injury, the suppression of miR-188-3p was enhanced by the overexpression of Mbd2-AL1; however, this effect was reversed by Mbd2-AL1 siRNA. Second, the FISH results indicated that Mbd2-AL1 and miR-188-3p colocalized in the cytoplasm of RGCs. Finally, the luciferase reporter assay further confirmed their interaction. In addition, the role of miR-188-3p in cell apoptosis remains controversial. One study demonstrated that miR-188-3p suppressed the apoptosis of spermatogenic cells.[21] However, another study reported that miR-188-3p promoted neuroapoptosis and cognitive impairments in animals.[36] In the current study, we found that miR-188-3p inhibits RGC apoptosis induced by I/R injury. To further clarify the anti-apoptosis mechanism of miR-188-3p, we focused on an apoptosis inducer of Traf3.[22] First, we predicted that Traf3 was the target of miR-188-3p. Subsequently, the luciferase reporter assay confirmed that miR-188-3p directly binds to the 3′ UTR region of Traf3. In addition, the overexpression of miR-188-3p suppressed Traf3 mRNA and protein expression levels and later mediated RGC apoptosis during I/R injury. Finally, the miR-188-3p inhibitor reversed the anti-apoptosis effect of Mbd2-AL1 siRNA following ischemic injury. Interestingly, Mbd2-KO mice significantly suppressed the Mbd2-AL1/miR-188-3p/Traf3 axis. Taken together, these results demonstrated that the Mbd2/Mbd2-AL1/miR-188-3p/Traf3 axis was responsible for RGC apoptosis during I/R injury.

In summary, our data demonstrated that Mbd2 mediated I/R-induced RGC apoptosis in primary RGCs and mice. Mechanistically, Mbd2 promoted the expression of lncRNA Mbd2-AL1 through promoter hypomethylation, leading to the inhibition of miR-188-3p expression, which prevented Traf3 downregulation. Taken together, the data suggest that Mbd2 may be a pivotal therapeutic target in retinal ischemic reperfusion injury.

MATERIALS AND METHODS

Ethics Statement

Mbd2 global knockout mice were purchased from Cyagen Biosciences (Guangzhou, People's Republic of China). All of the experiments were carried out in accordance with a protocol approved by the Animal Care and Use Committee of the Second Xiangya Hospital, Central South University in China.

Animals

Mice were housed under a 12:12-h light/dark cycle and were allowed free access to water and food. C57BL/6J mice (Jackson Laboratory) were used as wide-type (WT) controls. Experimental interventions were conducted under anesthesia using intraperitoneally injected solution of ketamine (100 mg/kg body weight; Ratiopharm, Ulm, Germany) and xylazine (5 mg/kg; Bayer Vital, Leverkusen, Germany). All animals were directly and daily observed after each intervention to ensure adequate health conditions and general behaviors.

Ischemia/Reperfusion Model

Mice were anesthetized as described above. Corneal analgesia was achieved with topical drops of 0.4% oxybuprocaine hydrochloride (Santen Pharmaceutical, Japan). Retinal I/R injuries were carefully established by cannulation of the cornea in the right eyes with a 33-gauge infusion needle that was connected to a plastic container of 200 mL sterile saline solution (0.9%) and as was described in previous methods.[5,37] The intraocular pressure was raised to 120 mmHg (measured with the TonoLab) for 60 min by elevating the saline container, followed by reperfusion in mice. The contralateral eye was cannulated and maintained at normal intraocular pressure to serve as a control. Retinal ischemia was confirmed

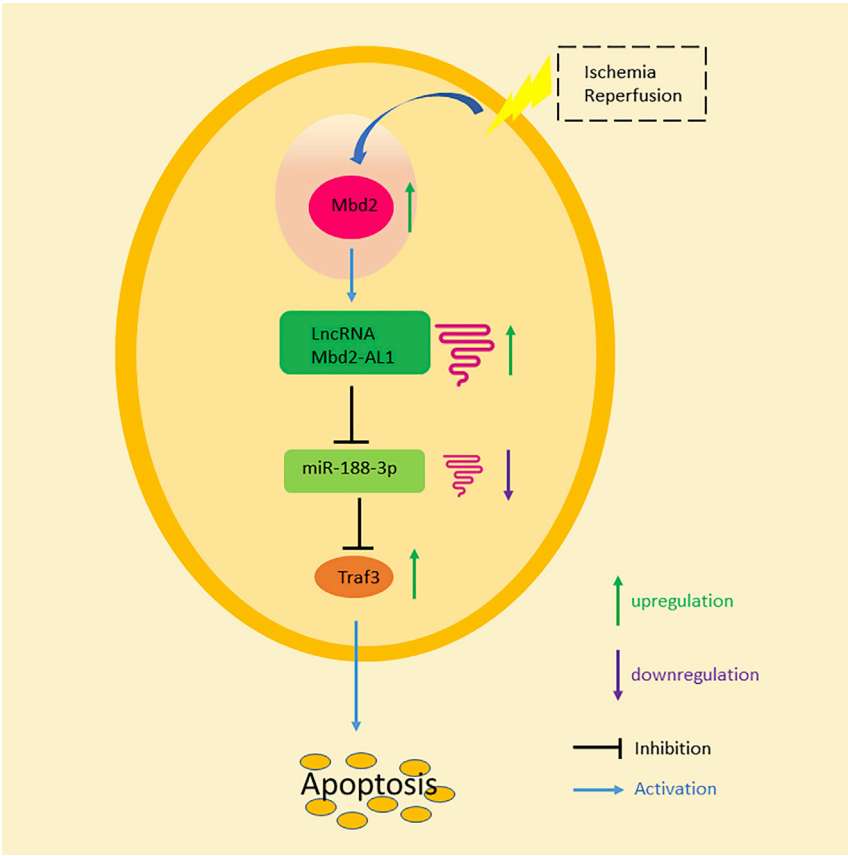

Figure 12. Schematic Diagram Summarizing the Role of Mbd2 in I/R-Induced RGC Apoptosis

In retinal I/R, Mbd2 promotes the transcription of Mbd2-AL1 via the hypomethylation of its promoter, which serves as a sponge that prevents miR-188-3p from mediating the downregulation of Traf3, which eventually leads to RGC apoptosis.

by whitening of the iris and loss of red reflex and subsequent reperfusion by the return of the red reflex. During the experiment, the body temperature was maintained on a temperature-controlled heat pad at 37°C. After needle removal, 0.3% tobramycin and 0.1% dexamethasone eye ointment (Alcon Cusi, Spain) were applied to the conjunctival sac. The mice were killed by CO_2 inhalation under anesthesia. Animal experiments were performed in accordance with a protocol approved by the Institutional Committee for the Care and Use of Laboratory Animals of the Second Xiangya Hospital, China.

Isolation and Culture of RGCs

Primary RGCs were isolated from the retina of 1- to 4-day postnatal newborn mice of either sex, as reported in previous studies, but with a partial modification.[16,38] All procedures were carried out under aseptic conditions. The day before dissection of the retina, we prepared a poly-d-lysine (Sigma; P6407)- and laminin (Sigma; L-6274)-coated 24-well plate; purified donkey anti-rabbit immunoglobulin G (IgG; heavy-chain [H] and light-chain [L])-coated, 75-cm^2 cell-culture dish for anti-macrophage panning; and donkey anti-rat IgG (H and L)-coated, 100-cm^2 dish for Thy1.2 antibody. An amount of 5 mL Dulbecco's PBS (DPBS) containing 30 μL Thy1.2 antibody (Sigma; M7898) was added to a 100-cm^2 dish before use. The retinas were washed in DPBS using a pipette and transferred to a papain solution for incubation at 37°C for 15 min. Low ovomucoid plus rabbit anti-mouse microphage antibody was added and incubated for 5 min at room temperature (RT) for macrophage binding. A panning buffer was added to bring up the volume, and the cell suspension was removed to the previously prepared anti-macrophage flask and incubated for 40 min at RT. The flask was gently shaken, and the cells were filtered through a Nitex mesh into an autoclaved beaker. The cell suspension was transferred to a Thy1.2 dish for 1 h, nonadherent cells were discarded, and 4 mL trypsin/Earle's balanced salt solution (EBSS) was added to digest RGCs off the plate. An amount of 80 μL was removed for cell counting and viability assessment, and the rest of the solution was centrifuged at 200 *g* for 5 min. The cell pellet was resuspended in pre-equilibrated RGC growth media. Laminin was removed from the poly-D-lysine-coated culture dish, and the cells were added with culture medium. RGCs were cultured in moist air with 5% of CO_2 and 95% O_2 at 37°C. 50% of medium was removed and replaced with prewarmed whole-growth medium every 3 days. (More details of reagents can be seen in the Supplemental Information.)

Cell viability was determined with a cytotoxicity staining kit (Live/Dead; Molecular Probes). The live cells cleaved calcein, yielding green fluorescence; the nucleic acids of the dead cells were labeled with red fluorescence using ethidium D. The cells were counted with the inverted microscope Leica DMI3000B, equipped with fluorescence illumination.

In Vitro Ischemia Simulation and Transfection of RGCs

The ischemic model of RGCs was made according to the previously published study.[39] Briefly, as RGCs were over 90 percent confluent, the media were changed to Hanks' balanced salt solution (HBSS), with 10 μM antimycin A (a complex III inhibitor of mitochondrial electron transport; ab141904; Abcam, Cambridge, MA, US) and 2 μM calcium ionophore (A2318; Aladdin, Shanghai, China), which were dissolved in dimethylsulfoxide (DMSO) for 2 h. The whole-growth medium was retrieved and sustained for 0 h to 4 h. Lipofectamine 2000 was applied for the transfection of 50 nM of Mbd2 siRNA, Mbd2-AL1 siRNA, Traf3 siRNA, plasmid of Mbd2, Mbd2-AL1, and miR-188-3p mimic or inhibitor (Ribobio, Guangzhou, China), 24 h before ischemia treatment and following the manufacturer's instruction.

Flow Cytometry Analysis of Apoptosis

Cell apoptosis was detected using the Annexin V/propidium iodide (PI) staining kit. Fluorescein isothiocyanate (FITC; #556547) and phycoerythrin (PE; #559763) Annexin V Apoptosis Detection Kit I was purchased from BD Biosciences (Franklin Lake, NJ, US). RGCs were trypsinized with 0.25% trypsin and washed twice with cold PBS and then resuspended in one time binding buffer at a concentration of 1×10^6 cells/mL. 100 μL from the above solution was transferred to a 5-mL culture tube, and 5 μL FITC Annexin V (or PE Annexin V) and 5 μL PI (or 7-aminoactinomycin D [7-AAD]) were added. The cells were gently vortexed and incubated for 15 min at RT (25°C) and in the dark. A 400-μL one time binding buffer was added to each tube. Flow cytometry was conducted, and the data were analyzed using FACSCalibur and FlowJo V10 software within 1 h.

Western Blotting

Retina tissues and cells were lysed using a lysis buffer (125 mM HCl [pH 6.8], 4% SDS, 20% glycerol, urea 0.36 g/mL, 20 mM DTT, 1% proteinase inhibitor cocktail), and the proteins were resuspended in SDS-PAGE loading buffer. Equal amounts of samples were loaded in each lane. The proteins were separated in 12% polyacrylamide gels and transferred to polyvinylidene difluoride (PVDF) membranes. The blots were then probed with primary antibodies against Mbd2 (GenBank: 17191) (#ab188474; Abcam, Cambridge, MA, US), caspase3/cleaved caspase3 (#9662; CST, Danvers, MA, US), Traf3 (GenBank: 22031) (#ab36988; Abcam), and β-tubulin (#10094-1-AP; Proteintech, Rosemont, IL, US), followed by incubation with species-specific horseradish peroxidase-conjugated secondary antibodies (goat anti-rabbit IgG, SA00001-2; Proteintech), and visualized by enhanced chemiluminescence (Millipore; WBKLSO500). Finally, the images were captured by Tanon 5200 Multi. The target proteins were quantified by Photoshop software and normalized by internal control β-tubulin to get relative expression levels.

Quantitative Real-Time PCR

Total RNA from retinas and RGCs were extracted using Trizol reagent (Invitrogen, Carlsbad, CA, US), according to the manufacturer's protocol. Approximately 40 ng total RNA was reverse transcribed using the PrimeScript RT Reagent Kit and genomic DNA (gDNA) Eraser Kit (RR047A; Takara, Dalian, Liaoning, China). The expression levels of lncRNAs, miRNAs, and mRNAs were detected using SYBR Green (#K0221; Thermo Scientific, Waltham, MA, US), and the ΔCt value was calculated and obtained using StepOne software (Bio-Rad, Hercules, CA, US). The sequences of lncRNA Mbd2-AL1 and miR-188-3p were retrieved from GenBank database (GenBank: 67895 and GenBank: 387183, respectively). Primer sequences were included in Table S3.

ChIP Analysis

The Chromatin Immunoprecipitation Kit (#17-371RF; Millipore, MA, US) was used to analyze the interaction between Mbd2 and relevant lncRNAs following the manufacturer's instructions. In brief, 37% formaldehyde (or fresh 18.5% formaldehyde) was added into the cell growth media to cross link the proteins to the DNA. Then, the cells were lysed and sonicated to obtain 200 bp- to 1,000 bp-length crosslinked DNA. Anti-Mbd2 antibody was used to pull down the immunoprecipitate (IP) of crosslinked protein/DNA at 4°C, incubating overnight. 60 μL of protein G agarose was added to each IP and incubated for 1 h at 4°C, with rotation to collect the antibody/antigen/DNA complex. Afterward, protein/DNA complexes were eluted, and the crosslinks reversed between protein/DNA complexes to free DNA. Finally, a spin column was used to bind free DNA onto filter paper discs for DNA purification. The precipitated DNAs were detected by PCR using specific mBS1-5 primers (Table S3).

Luciferase Reporter Assay

The Dual-Luciferase Reporter Assay System Kit (E1910) was purchased from Promega (Madison, WI, US). On one hand, we constructed pCpGfree-basic-Lucia (pCpGl) reporter (Invivogen, San Diego, CA, US; #pcpgf-basic) that contained CG DNA methylation target sequences in the promoter region of lncRNA Mbd2-AL1, which was cotransfected with Mbd2 or mtMbd2 (mutational Mbd2, depletion of DNA methylation domain) plasmids and the renilla plasmid. On the other hand, dual-luciferase reporter (firefly luciferase-renilla luciferase double labeled) of lncRNA Mbd2-AL1-WT or -MUT and Traf3-WT or -MUT (mutation) at 3′ UTR regions was constructed and cotransfected with the miR-188-3p mimic, and the cells were lysed by passive lysis buffer, 48 h later. Luciferase Assay Reagent II (LAR II) was added and the firefly luciferase levels detected. Stop & Glo Reagent (substrate + buffer) to measure the renilla luciferase values was added. Finally, luciferase levels were normalized by renilla luciferase values to obtain final results. The plasmids above were constructed by RuQi Biotechnology (Guangzhou, Guangdong, China).

Fluorescence *In Situ* Hybridization (FISH)

For FISH analysis, the Fluorescent *In Situ* Hybridization Kit (C10910; Ribobio, Guangzhou, China) was used. Briefly, RGCs were fixed in paraformaldehyde and hybridized overnight at 37°C with miR-188-3p and lncRNA Mbd2-AL1 probes (Ribobio, Guangzhou, China) in hybridization buffer, and the cell nuclei were stained with 4′,6-diamidino-2-phenylindole (DAPI). Fluorescence images were captured using a laser-scanning confocal microscope (Nikon; Eclipse Ti), and the images were conducted by Eclipse C2 (Nikon, Tokyo, Japan).

Immunofluorescence and TUNEL Assay

Following I/R injury, the mice were sacrificed at time intervals of 6 h, 12 h, 24 h, 48 h, and 7 days. The eyes were immediately enucleated, treated with 4% paraformaldehyde for 1 h, and the anterior section was removed. Then, the eye cups were put in FAS eye-fixation buffer (Servicebio; G1109) at 4°C overnight and dehydrated in 30% source solution. Eye cups were embedded in OCT (optimum cutting temperature compound) and frozen at −80°C. 10 μm-thick cryosections of eye cups were obtained by a freezing microtome. All of the sections were permeabilized and blocked (10% BSA, 0.1% Triton X-100 in

PBS) for 1 h. Eye sections were incubated with primary antibodies at 4°C overnight, followed by 2 h incubations at RT in the dark with the secondary antibodies CY3-goat anti-rabbit IgG (BA1032; Boster, Wuhan, China) and goat anti-rabbit IgG H and L (Alexa Fluor 488, ab150077; Abcam). The nuclei were visualized with DAPI. Retina whole mount was treated as before, but in this case, the retinas, instead of the eye cups, were dissected. The retinas were permeabilized with a higher concentration of Triton X-100 at 10%, and a terminal-deoxy-transferase-mediated 2′-deoxyuridine, 5′-triphosphate (dUTP) nick end-labeling (TUNEL) (#1684795; Roche, Basel, Switzerland) assay was performed, according to the manufacturer's instructions, to detect apoptotic RGCs in the retinas. Briefly, cryosections were permeabilized and incubated with TUNEL solution (including 50 μL enzyme solution [terminal deoxynucleotidyl transferase (TdT)] and 450 μL label solution [fluorescein-dUTP]) at 37°C for 1 h and then washed with PBS and stained with DAPI.

Electroretinography

As it was reported that a diminished b-wave was a sensitive marker of ischemic injury,[40] we evaluated retinal function by ERG in mice. ERG was performed at 0 h, 48 h, and 7 days after ischemia. After at least 6 h of dark adaptation, the animals were anesthetized and prepared for recording, as previously described. Briefly, the animals were placed in a specially designed dome with body temperature maintained at 37°C. The corneas were anesthetized with a topical 0.4% oxybuprocaine hydrochloride, and the pupils were dilated with 1% tropicamide. Five electrodes were separately applied to the subcutaneous tissue by the tails, beneath each eye, and at the apex of the corneas of the two eyes. Each eye was exposed to light flashes at a series of intensity (0.01, 3, and 10 cd.s/m^2). The amplitudes and implicit times of waveforms were measured and analyzed.[41]

Statistical Analysis

All data values were expressed as mean ± standard deviations of the mean (SEM). One-way ANOVA, followed by the Tukey's post-hoc test was used to compare multiple treatment groups. Two-way ANOVA was used to assess the statistical significance of the differences between multiple treatment groups at different time points. Data were expressed as mean ± SEM of five independent experiments. The results were statistically significant when $p < 0.05$.

SUPPLEMENTAL INFORMATION

Supplemental Information can be found online at https://doi.org/10.1016/j.omtn.2020.01.011.

AUTHOR CONTRIBUTIONS

H.Li. designed the research and revised the manuscript. Y.Ge. performed the experiments and wrote the manuscript. R.Zhang. collected data and did the statistical analysis. Y.Feng. purchased the reagents and assembled the figures.

CONFLICTS OF INTEREST

The authors declare no competing interests.

ACKNOWLEDGMENTS

This work was supported by the National Natural Science Foundation of China (81770951), the Hunan Province Natural Science Foundation (2018JJ2568), and the Fundamental Research Funds for the Central Universities of Central South University (2019zzts1046).

REFERENCES

1. Kergoat, H., Hérard, M.E., and Lemay, M. (2006). RGC sensitivity to mild systemic hypoxia. Invest. Ophthalmol. Vis. Sci. *47*, 5423–5427.
2. Osborne, N.N., Casson, R.J., Wood, J.P., Chidlow, G., Graham, M., and Melena, J. (2004). Retinal ischemia: mechanisms of damage and potential therapeutic strategies. Prog. Retin. Eye Res. *23*, 91–147.
3. Schmid, H., Renner, M., Dick, H.B., and Joachim, S.C. (2014). Loss of inner retinal neurons after retinal ischemia in rats. Invest. Ophthalmol. Vis. Sci. *55*, 2777–2787.
4. Almasieh, M., Wilson, A.M., Morquette, B., Cueva Vargas, J.L., and Di Polo, A. (2012). The molecular basis of retinal ganglion cell death in glaucoma. Prog. Retin. Eye Res. *31*, 152–181.
5. L, H., Zhu, X., Fang, F., Jiang, D., and Tang, L. (2014). Down-regulation of GRP78 enhances apoptosis via CHOP pathway in retinal ischemia-reperfusion injury. Neurosci. Lett. *575*, 68–73.
6. Corso-Diaz, X., Jaeger, C., Chaitankar, V., and Swaroop, A. (2018). Epigenetic control of gene regulation during development and disease: a view from the retina. Prog. Retin. Eye Res. *65*, 1–27.
7. Ginder, G.D., and Williams, D.C., Jr. (2018). Readers of DNA methylation, the MBD family as potential therapeutic targets. Pharmacol. Ther. *184*, 98–111.
8. Rhee, K.D., Yu, J., Zhao, C.Y., Fan, G., and Yang, X.-J. (2012). Dnmt1-dependent DNA methylation is essential for photoreceptor terminal differentiation and retinal neuron survival. Cell Death Dis. *3*, e427.
9. Smith, Z.D., and Meissner, A. (2013). DNA methylation: roles in mammalian development. Nat. Rev. Genet. *14*, 204–220.
10. Wang, J., Li, H., Qiu, S., Dong, Z., Xiang, X., and Zhang, D. (2017). MBD2 upregulates miR-301a-5p to induce kidney cell apoptosis during vancomycin-induced AKI. Cell Death Dis. *8*, e3120.
11. Ushijima, T., Nakajima, T., and Maekita, T. (2006). DNA methylation as a marker for the past and future. J. Gastroenterol. *41*, 401–407.
12. Rao, X., Zhong, J., Zhang, S., Zhang, Y., Yu, Q., Yang, P., Wang, M.H., Fulton, D.J., Shi, H., Dong, Z., et al. (2011). Loss of methyl-CpG-binding domain protein 2 enhances endothelial angiogenesis and protects mice against hind-limb ischemic injury. Circulation *123*, 2964–2974.
13. Esteller, M. (2011). Non-coding RNAs in human disease. Nat. Rev. Genet. *12*, 861–874.
14. Fatica, A., and Bozzoni, I. (2014). Long non-coding RNAs: new players in cell differentiation and development. Nat. Rev. Genet. *15*, 7–21.
15. Morris, K.V., and Mattick, J.S. (2014). The rise of regulatory RNA. Nat. Rev. Genet. *15*, 423–437.
16. Yao, J., Wang, X.Q., Li, Y.J., Shan, K., Yang, H., Wang, Y.N., Yao, M.D., Liu, C., Li, X.M., Shen, Y., et al. (2016). Long non-coding RNA MALAT1 regulates retinal neurodegeneration through CREB signaling. EMBO Mol. Med. *8*, 346–362.
17. Cai, Y., Yu, X., Hu, S., and Yu, J. (2009). A brief review on the mechanisms of miRNA regulation. Genomics Proteomics Bioinformatics *7*, 147–154.
18. Paraskevopoulou, M.D., and Hatzigeorgiou, A.G. (2016). Analyzing MiRNA-LncRNA Interactions. Methods Mol. Biol. *1402*, 271–286.
19. Wang, K.C., and Chang, H.Y. (2011). Molecular mechanisms of long noncoding RNAs. Mol. Cell *43*, 904–914.
20. Wang, K., Long, B., Zhou, L.Y., Liu, F., Zhou, Q.-Y., Liu, C.-Y., Fan, Y.-Y., and Li, P.-F. (2014). CARL lncRNA inhibits anoxia-induced mitochondrial fission and apoptosis in cardiomyocytes by impairing miR-539-dependent PHB2 downregulation. Nat. Commun. *5*, 3596.

21. Song, W.-Y., Meng, H., Wang, X.-G., Jin, H.X., Yao, G.D., Shi, S.L., Wu, L., Zhang, X.Y., and Sun, Y.P. (2017). Reduced microRNA-188-3p expression contributes to apoptosis of spermatogenic cells in patients with azoospermia. Cell Prolif. *50*, e12297.

22. Georgopoulos, N.T., Steele, L.P., Thomson, M.J., Selby, P.J., Southgate, J., and Trejdosiewicz, L.K. (2006). A novel mechanism of CD40-induced apoptosis of carcinoma cells involving TRAF3 and JNK/AP-1 activation. Cell Death Differ. *13*, 1789–1801.

23. Tokarz, P., Kaarniranta, K., and Blasiak, J. (2016). Inhibition of DNA methyltransferase or histone deacetylase protects retinal pigment epithelial cells from DNA damage induced by oxidative stress by the stimulation of antioxidant enzymes. Eur. J. Pharmacol. *776*, 167–175.

24. Wahlin, K.J., Enke, R.A., Fuller, J.A., Kalesnykas, G., Zack, D.J., and Merbs, S.L. (2013). Epigenetics and cell death: DNA hypermethylation in programmed retinal cell death. PLoS One *8*, e79140.

25. Weaver, I.C., Hellstrom, I.C., Brown, S.E., Andrews, S.D., Dymov, S., Diorio, J., Zhang, T.Y., Szyf, M., and Meaney, M.J. (2014). The methylated-DNA binding protein MBD2 enhances NGFI-A (egr-1)-mediated transcriptional activation of the glucocorticoid receptor. Philos. Trans. R. Soc. Lond. B Biol. Sci. *369*, 20130513.

26. Zhang, X., Shi, E., Yang, L., Fu, W., Hu, F., and Zhou, X. (2019). LncRNA AK077216 is downregulated in diabetic retinopathy and inhibited the apoptosis of retinal pigment epithelial cells by downregulating miR-383. Endocr. J. *66*, 1011–1016.

27. Wan, P., Su, W., Zhang, Y., Li, Z., Deng, C., Li, J., Jiang, N., Huang, S., Long, E., and Zhuo, Y. (2020). LncRNA H19 initiates microglial pyroptosis and neuronal death in retinal ischemia/reperfusion injury. Cell Death Differ. *27*, 176–191.

28. Tong, P., Peng, Q.H., Gu, L.M., Xie, W.-W., and Li, W.-J. (2019). LncRNA-MEG3 alleviates high glucose induced inflammation and apoptosis of retina epithelial cells via regulating miR-34a/SIRT1 axis. Exp. Mol. Pathol. *107*, 102–109.

29. Miao, X., and Liang, A. (2019). Knockdown of long noncoding RNA GAS5 attenuates H_2O_2 -induced damage in retinal ganglion cells through upregulating miR-124: Potential role in traumatic brain injury. J. Cell. Biochem. *120*, 2313–2322.

30. Li, C.P., Wang, S.H., Wang, W.Q., Song, S.G., and Liu, X.M. (2017). Long Noncoding RNA-Sox2OT Knockdown Alleviates Diabetes Mellitus-Induced Retinal Ganglion Cell (RGC) injury. Cell. Mol. Neurobiol. *37*, 361–369.

31. Li, H.B., You, Q.S., Xu, L.X., Sun, L.-X., Majid, A.S.A., Xia, X.-B., and Ji, D. (2017). Long Non-Coding RNA-MALAT1 Mediates Retinal Ganglion Cell Apoptosis Through the PI3K/Akt Signaling Pathway in Rats with Glaucoma. Cell. Physiol. Biochem. *43*, 2117–2132.

32. Yan, B., Yao, J., Liu, J.-Y., Li, X.M., Wang, X.Q., Li, Y.J., Tao, Z.F., Song, Y.C., Chen, Q., and Jiang, Q. (2015). lncRNA-MIAT regulates microvascular dysfunction by functioning as a competing endogenous RNA. Circ. Res. *116*, 1143–1156.

33. Wu, X.-Z., Cui, H.-P., Lv, H.-J., and Feng, L. (2019). Knockdown of lncRNA PVT1 inhibits retinoblastoma progression by sponging miR-488-3p. Biomed. Pharmacother. *112*, 108627.

34. Zhang, L., Dong, Y., Wang, Y., Gao, J., Lv, J., Sun, J., Li, M., Wang, M., Zhao, Z., Wang, J., and Xu, W. (2019). Long non-coding RNAs in ocular diseases: new and potential therapeutic targets. FEBS J. *286*, 2261–2272.

35. Wang, X., Zhang, X., Han, Y., Wang, Q., Ren, Y., Wang, B., and Hu, J. (2019). Silence of lncRNA ANRIL represses cell growth and promotes apoptosis in retinoblastoma cells through regulating miR-99a and c-Myc. Artif. Cells Nanomed. Biotechnol. *47*, 2265–2273.

36. Wang, L., Zheng, M., Wu, S., and Niu, Z. (2018). MicroRNA-188-3p is involved in sevoflurane anesthesia-induced neuroapoptosis by targeting MDM2. Mol. Med. Rep. *17*, 4229–4236.

37. Kim, B.J., Braun, T.A., Wordinger, R.J., and Clark, A.F. (2013). Progressive morphological changes and impaired retinal function associated with temporal regulation of gene expression after retinal ischemia/reperfusion injury in mice. Mol. Neurodegener. *8*, 21.

38. Barres, B.A., Silverstein, B.E., Corey, D.P., and Chun, L.L. (1988). Immunological, morphological, and electrophysiological variation among retinal ganglion cells purified by panning. Neuron *1*, 791–803.

39. Lee, H.T., and Emala, C.W. (2002). Preconditioning and adenosine protect human proximal tubule cells in an in vitro model of ischemic injury. J. Am. Soc. Nephrol. *13*, 2753–2761.

40. Grozdanic, S.D., Sakaguchi, D.S., Kwon, Y.H., Kardon, R.H., and Sonea, I.M. (2003). Functional characterization of retina and optic nerve after acute ocular ischemia in rats. Invest. Ophthalmol. Vis. Sci. *44*, 2597–2605.

41. Silverman, S.M., Kim, B.-J., Howell, G.R., Miller, J., John, S.W., Wordinger, R.J., and Clark, A.F. (2016). C1q propagates microglial activation and neurodegeneration in the visual axis following retinal ischemia/reperfusion injury. Mol. Neurodegener. *11*, 24.

OMTN, Volume *19*

Supplemental Information

Mbd2 Mediates Retinal Cell Apoptosis by Targeting the lncRNA Mbd2-AL1/miR-188-3p/Traf3 Axis in Ischemia/Reperfusion Injury

Yanni Ge, Ran Zhang, Yuqing Feng, and Huiling Li

Mbd2 mediates retinal cell apoptosis by targeting the lncRNA Mbd2-AL1/miR-188-3p/Traf3 axis in ischemia/reperfusion injury

Yanni Ge, Ran Zhang, Yuqing Feng, Huiling Li

Supplementary Table 1. upregulated lncRNAs in Scramble/I/R group vs. Scramble group

upregulated lncRNAs in Scramble/I/R group vs. Scramble group		
ENSMUST00000163697	ENSMUST00000180630	ENSMUST00000125004
ENSMUST00000123078	uc.129-	ENSMUST00000149283
AK039484	ENSMUST00000154204	ENSMUST00000138771
ENSMUST00000181828	AK051538	ENSMUST00000141071
ENSMUST00000136537	AK048741	mouselincRNA0767+
ENSMUST00000145757	ENSMUST00000124091	ENSMUST00000130983
NR_040420	ENSMUST00000160677	AK048998
AK138545	ENSMUST00000135399	mouselincRNA0543-
ENSMUST00000171450	TCONS_00012085	ENSMUST00000140873
uc009ljz.1	AK020950	uc008eew.1
ENSMUST00000149302	ENSMUST00000146069	ENSMUST00000173538
humanlincRNA0561-	AK003980	AK016924
uc007clk.1	uc.64+	ENSMUST00000147045
ENSMUST00000149054	uc029soj.1	ENSMUST00000099260
ENSMUST00000141528	AK144529	ENSMUST00000162149
uc.252-	AK081864	ENSMUST00000133880
AK155686	ENSMUST00000169387	ENSMUST00000127429
AK142692	uc009hik.1	ENSMUST00000140754
AK134910	ENSMUST00000124653	AK046972
AK154589	AK082284	NR_028263
uc.34-	ENSMUST00000125409	uc009dqv.1
AK032419	ENSMUST00000142248	ENSMUST00000181830
humanlincRNA1945-	uc.19-	ENSMUST00000152860
ENSMUST00000129027	ENSMUST00000135495	ENSMUST00000160516
ENSMUST00000129502	ENSMUST00000174338	AK086566
AK140140	ENSMUST00000099647	ENSMUST00000143806
ENSMUST00000120404	ENSMUST00000149030	NR_102293
uc.250-	ENSMUST00000161623	uc007ees.1
AK139938	uc007ihz.1	ENSMUST00000131987
NR_033526	uc029rkv.1	ENSMUST00000139847
AK040434	ENSMUST00000130883	ENSMUST00000125867
ENSMUST00000129096	AK039081	ENSMUST00000133539
uc009euf.1	AK079872	ENSMUST00000124624
ENSMUST00000146327	uc.426-	ENSMUST00000152779
ENSMUST00000176431	ENSMUST00000167053	TCONS_00025263

AK003907	ENSMUST00000142818	uc009avw.1
ENSMUST00000139786	ENSMUST00000156701	ENSMUST00000180544
AK132438	AK139467	ENSMUST00000137683
mouselincRNA1097-	ENSMUST00000177480	AK030568
AK030243	ENSMUST00000180982	NR_040746
humanlincRNA0635+	ENSMUST00000143129	ENSMUST00000137043
AK144133	TCONS_00015979	TCONS_00015184
ENSMUST00000159153	AK156905	ENSMUST00000180757
ENSMUST00000119517	ENSMUST00000120603	ENSMUST00000176773
TCONS_00036126	humanlincRNA0194+	ENSMUST00000159700
AK157120	AK047632	AK085151
ENSMUST00000149420	uc.461+	ENSMUST00000161664
ENSMUST00000149692	ENSMUST00000169214	ENSMUST00000123946
ENSMUST00000180460	ENSMUST00000159117	ENSMUST00000051531
uc012fvb.1	ENSMUST00000127068	ENSMUST00000065709
ENSMUST00000126912	AK032249	ENSMUST00000110954
AK047380	ENSMUST00000171273	ENSMUST00000026264
ENSMUST00000126846	AK033143	ENSMUST00000151023
AK009126	mouselincRNA1098+	ENSMUST00000147329
AK140706	uc.247+	ENSMUST00000153000
ENSMUST00000159399	AK042899	uc007ktl.1
ENSMUST00000135931	ENSMUST00000135601	AK148890
AK043360	AK020372	ENSMUST00000134755
ENSMUST00000163665	humanlincRNA0650-	ENSMUST00000140514
ENSMUST00000155086	ENSMUST00000159037	NR_045176
ENSMUST00000154578	uc.367+	ENSMUST00000181302
AK020279	ENSMUST00000153863	AK040345
ENSMUST00000176131	ENSMUST00000181514	humanlincRNA1605+
uc.77-	ENSMUST00000167073	uc007pkb.2
NR_045542	AK142125	uc009dml.1
AK046984	ENSMUST00000163081	ENSMUST00000155728
AK052120	ENSMUST00000144793	uc.74-
ENSMUST00000137375	AK089653	AK143399
ENSMUST00000132787	mouselincRNA1511-	AK034976
ENSMUST00000180819	AK157323	ENSMUST00000133112
AK041489	CF616316	ENSMUST00000143340
ENSMUST00000154896	TCONS_00034053	AK015830
AK018645	NR_029382	NR_030675
NR_015467	uc007rvk.1	ENSMUST00000122109
ENSMUST00000148857	AK054326	ENSMUST00000160470
AK089422	ENSMUST00000133365	ENSMUST00000162801
ENSMUST00000107148	NR_045640	ENSMUST00000156295

uc007baf.1	AK156102	ENSMUST00000172812
ENSMUST00000159157	ENSMUST00000142932	ENSMUST00000174520
ENSMUST00000149805	ENSMUST00000173251	uc029sug.1
ENSMUST00000147861	AK040898	AK045182
ENSMUST00000151257	ENSMUST00000132434	ENSMUST00000145421
uc007zgf.1	AK047864	uc008elz.1
AK052777	ENSMUST00000130038	AK081208
TCONS_00013499	ENSMUST00000152600	uc007txt.1
AK142735	AK039385	ENSMUST00000139702
AK148874	ENSMUST00000147654	AK028736
TCONS_00003993	AK020425	ENSMUST00000125424
ENSMUST00000159393	ENSMUST00000156145	ENSMUST00000118822
AK037099	ENSMUST00000160159	TCONS_00009802
TCONS_00006732	ENSMUST00000136126	ENSMUST00000127318
ENSMUST00000181422	ENSMUST00000145728	AK035280
ENSMUST00000136610	AK037210	AK013121
uc029wtn.1	uc029xdn.1	uc007sgd.1
ENSMUST00000177445	AK031651	ENSMUST00000163608
uc009ril.1	BY573946	AK016790
ENSMUST00000125326	NR_015610	AK153797
ENSMUST00000144231	ENSMUST00000155767	uc.335+
AK140170	ENSMUST00000140461	ENSMUST00000067521
AK045044	uc.276+	NR_040295
ENSMUST00000120786	AK153393	AK085385
ENSMUST00000146281	uc012gti.1	ENSMUST00000143841
AK049728	humanlincRNA0518+	AK082454
TCONS_00025329	ENSMUST00000139607	AK038145
ENSMUST00000151412	ENSMUST00000124559	AK045073
ENSMUST00000151582	ENSMUST00000141336	ENSMUST00000155423
ENSMUST00000140602	ENSMUST00000162912	AK043671
AK155038	TCONS_00009665	AK132396
AK079498	humanlincRNA0043+	uc007dlv.1
AK133451	uc007ssb.1	AK043028
ENSMUST00000161580	uc008hdz.1	ENSMUST00000181387
AK089789	ENSMUST00000123262	AK142149
AK020824	ENSMUST00000154706	uc011zox.1
ENSMUST00000130441	AK077872	uc007ydb.1
ENSMUST00000128766	ENSMUST00000161769	humanlincRNA1178+
ENSMUST00000180281	ENSMUST00000122281	ENSMUST00000180377
AK140232	ENSMUST00000140487	ENSMUST00000149117
uc007dtm.1	AK142657	ENSMUST00000118579
ENSMUST00000118575	AK052802	AK135681

ENSMUST00000157701	AK037904	NR_027952
ENSMUST00000156396	ENSMUST00000144292	AK052126
ENSMUST00000129240	AK142890	uc009fbu.1
ENSMUST00000143025	ENSMUST00000162289	ENSMUST00000126627
humanlincRNA0933+	NR_039577	TCONS_00002220
ENSMUST00000155715	ENSMUST00000155761	ENSMUST00000137546
AK132891	ENSMUST00000154759	ENSMUST00000149299
ENSMUST00000132481	ENSMUST00000161304	ENSMUST00000156814
ENSMUST00000117697	2_00008059	ENSMUST00000181427
ENSMUST00000129374	NR_046233	AK018099
ENSMUST00000126446	humanlincRNA1907-	ENSMUST00000151468
ENSMUST00000148298	uc.275-	BM938732
AK037460	uc.195-	AK157381
AI390166	mouselincRNA0538-	AK144955
AK085893	ENSMUST00000150545	AK007047
uc.481-	ENSMUST00000156882	uc007qnc.1
ENSMUST00000176215	uc012coq.1	ENSMUST00000152911
ENSMUST00000181178	ENSMUST00000180919	AK133460
ENSMUST00000140231	AK016451	AK048415
ENSMUST00000144696	ENSMUST00000129260	

Supplementary Table 2. downregulated lncRNAs in MBD2 siRNA group

downregulated lncRNAs in MBD2 siRNA group		
ENSMUST00000177480	AK154589	ENSMUST00000099260
AK156905	AK052120	ENSMUST00000151412
AK016451	ENSMUST00000124091	ENSMUST00000122281
AK132396	ENSMUST00000162912	AK140140
AK156905	AK154589	ENSMUST00000180757
ENSMUST00000147654	uc029sug.1	AK140140
uc.247+	AK037904	ENSMUST00000137375
uc007zgf.1	ENSMUST00000137043	AK028736
ENSMUST00000135495	NR_033526	ENSMUST00000163697
NR_046233	ENSMUST00000151023	AK153393
TCONS_00002220	ENSMUST00000130883	ENSMUST00000163697
AK020372	AK132891	ENSMUST00000145728
ENSMUST00000154706	NR_033526	ENSMUST00000133880
AK018099	NR_045176	TCONS_00003993
TCONS_00006732	ENSMUST00000156701	ENSMUST00000119517
ENSMUST00000150545	ENSMUST00000120404	uc009hik.1
ENSMUST00000149299	AK054326	humanlincRNA0194+
ENSMUST00000142932	TCONS_00012085	ENSMUST00000140873

mouselincRNA0543-	AK133460	uc011zox.1
NR_040295	ENSMUST00000120404	uc007baf.1
ENSMUST00000118579	ENSMUST00000143806	ENSMUST00000180377
AK030243	TCONS_00025263	ENSMUST00000149117
NR_045640	ENSMUST00000181178	ENSMUST00000138771
ENSMUST00000163608	uc007ydb.1	uc012gti.1
AK135681	ENSMUST00000140461	NR_015467
ENSMUST00000129027	AK037460	AK155686
ENSMUST00000174520	ENSMUST00000067521	AK038145
ENSMUST00000144292	NR_039577	AK155686
AK081208	ENSMUST00000173538	mouselincRNA0767+
uc.276+	ENSMUST00000156396	AK018645
AK144529	ENSMUST00000124624	ENSMUST00000149054
uc.426-	ENSMUST00000148857	ENSMUST00000132481
ENSMUST00000180919	ENSMUST00000129096	ENSMUST00000180982
AK077872	ENSMUST00000136610	ENSMUST00000149054
BM938732	ENSMUST00000144231	ENSMUST00000149805
uc009fbu.1	uc009ril.1	BY573946
AK047632	ENSMUST00000129096	ENSMUST00000123078
ENSMUST00000155423	ENSMUST00000133112	ENSMUST00000144793
uc.335+	ENSMUST00000159117	AK042899
NR_102293	AK052126	AK047864
uc008hdz.1	AK007047	ENSMUST00000151582
ENSMUST00000172812	ENSMUST00000099260	ENSMUST00000132434
ENSMUST00000151412	ENSMUST00000135931	AK052777
ENSMUST00000136126	AK037210	uc009euf.1
ENSMUST00000128766	AK051538	ENSMUST00000181514
ENSMUST00000180281	ENSMUST00000137683	ENSMUST00000130983
ENSMUST00000156882	ENSMUST00000148298	uc.275-
ENSMUST00000143025	ENSMUST00000126627	uc009euf.1
ENSMUST00000135399	mouselincRNA1097-	NR_030675
AK082454	ENSMUST00000129502	ENSMUST00000149692
AK013121	AK140706	ENSMUST00000154578
AK048998	AK020824	ENSMUST00000181387
ENSMUST00000153863	AK134910	AK140170
ENSMUST00000143340	ENSMUST00000129502	uc029xdn.1
ENSMUST00000160470	AK140232	uc.64+
ENSMUST00000139607	ENSMUST00000181427	uc007ees.1
AK089653	ENSMUST00000125004	uc.367+
AK045182	NR_040746	ENSMUST00000136537
ENSMUST00000026264	ENSMUST00000143129	ENSMUST00000156701
ENSMUST00000141336	AK039484	ENSMUST00000147045

ENSMUST00000051531	AK142692	humanlincRNA0561-
ENSMUST00000126446	ENSMUST00000140514	ENSMUST00000161580
uc.195-	NR_028263	AK144133
AK020950	AK039484	AK030568
ENSMUST00000181828	AK142692	humanlincRNA0561-
ENSMUST00000155715	AK086566	ENSMUST00000129240
CF616316	ENSMUST00000162149	ENSMUST00000127429
AK043671	ENSMUST00000151468	ENSMUST00000149302
ENSMUST00000137546	AK034976	ENSMUST00000149302
ENSMUST00000123262	ENSMUST00000155728	NR_040420
AK043028	ENSMUST00000163665	ENSMUST00000181830
uc007rvk.1	AK031651	ENSMUST00000149302
ENSMUST00000150545	TCONS_00009802	ENSMUST00000147861
ENSMUST00000125326	ENSMUST00000110954	uc007ssb.1
ENSMUST00000156814	ENSMUST00000123946	AK016924
humanlincRNA1605+	AK039385	AK040434
TCONS_00015184	AK003980	AK039081
uc.481-	ENSMUST00000180630	AK046984
AK143399	ENSMUST00000129374	ENSMUST00000153000
ENSMUST00000176773	humanlincRNA0650-	ENSMUST00000127068
AK133451	ENSMUST00000135601	AK142657
uc009ljz.1	AK079872	TCONS_00034053
uc012coq.1	ENSMUST00000149283	ENSMUST00000145421
ENSMUST00000117697	ENSMUST00000099647	NR_015610
mouselincRNA1098+	TCONS_00015979	NR_045542
AK132438	ENSMUST00000107148	ENSMUST00000169387
ENSMUST00000147329	AK020279	ENSMUST00000140231
ENSMUST00000140602	AK049728	uc.252-
AK016790	ENSMUST00000126846	ENSMUST00000167073
ENSMUST00000161304	ENSMUST00000176131	ENSMUST00000157701
AK139467	ENSMUST00000155761	AK037099
uc029wtn.1	ENSMUST00000129260	uc007txt.1
humanlincRNA1178+	AK079498	AK032419
mouselincRNA1511-	ENSMUST00000127318	uc008eew.1
ENSMUST00000142818	AK081864	ENSMUST00000133365
AK032249	uc007ktl.1	AK041489
ENSMUST00000146327	ENSMUST00000146281	AI390166
AK089789	AK142735	ENSMUST00000176431
NR_027952	ENSMUST00000144696	AK082284
humanlincRNA0043+	ENSMUST00000118575	ENSMUST00000132787
ENSMUST00000145757	uc012fvb.1	ENSMUST00000130038
ENSMUST00000154204	AK144955	AK040345

ENSMUST00000167053	ENSMUST00000136537	AK142890
AK148890	ENSMUST00000159700	AK156102
AK085385	AK048415	uc008elz.1

Supplementary Table 3 primers of genes

Gene name	**Forward primer(5'to3')**	**Reverse primer(5'to3')**	**RT primer(5'to3')**
LncRNA Mbd2-AL1	AACTTGA AATCCCTCCTGTG CT	AGGCTTCAGTTCC AAACACTC	
miR-188-3p	CTCCCACATGCAG GGT	CAGTGC GTGTCGTGGAGT	GTCGTATCCAGTG CGTGTCGTGGAGT CGGCAATTGCACT GGATACGACTGCA AACC
Traf3	TCCAATTCCCTAA CCGCACC	GACCTGGGCTTGT AACCTCC	
GAPDH	CAA GGTCATCCATGAC AACTTTG	GTCCACCACCCTG TTGCTG TAG	
U6	CTCGCTTCGGCAG CACA	AACGCT TCACGAATTTGCG T	
mBS1	GGTGGTGTAATAG AATTA GGAAAATAAGT	CTAAAAATATACT ACCAACCCCC	
mBS2	GG TGGTGTAATAGAA TTAGGAAAATAAG T	AAAAATATACTAC CAACCC CC	
mBS3	GGTGTAATAGAAT TAGGAAAATAAGT T	AAATCTTC ATCTACCTCCCAA AAA	
mBS4	GGTGTAATAGAAT TAGGAAAATAAGT T	AAAACTAAAAATA TACTACCAACCCC C	
mBS5	GGTGGTGTA ATAGAATTAGGAA AATAAGT	TAAAAATATACTA CCAACCCCC	

Reagents of primary RGCs isolation

D-lysine (Sigma P6407);

laminin (Sigma L-6274);

Thy1.2 antibody (SIGMA M7898);

papain solution papain solution (Solarbio G8430), 2 mg L-cysteine (Sigma C-2529), 100 μl 0.4% DNase (Sigma D-4527) in 10 ml DPBS);

Lo Ovomucoid (including 600 mg BSA, 600 mg Trypsin inhibitor (ROCHE 4693159001) in 40 ml DPBS);

Rabbit anti-mouse microphage antibody (Accurate chemical AIA31240);

panning buffer (Add 2 ml DPBS/0.2% BSA to 18 ml DPBS. Add 200 μl insulin and 120 μg N-acetyl cysteine and 10ul Neurobasal);

RGC growth media (mainly containing Pen/Strep, insulin, sodium pyruvate, T3, L-glutamine, B27, BDNF, CNTF, Forskolin and bFGF, etc.)

Positive cells analysis in retina sections and whole-mount

For quantification, 10 randomly selected fields were observed in each section to count the TUNEL positive RGCs normalized to total nuclei in ganglion cell layer, 4 central retina slices were analyzed per animal. We quantified the number of cells in the ganglion cell layer (GCL) (in a blinded manner). The Statistician did not know the grouping condition of these retina samples. Images of retinal whole mounts were photographed from 2 different regions at the distance of 1 and 2 mm to the disc of each quadrant of the retina using a microscope of LEICA DMI3000B equipped with fluorescence illumination (Weztlar, Germany). Images were captured at a 20-fold magnification. Mean count of survival RGCs normalized to MBD2-WT/Sham group in 4 different groups. 8 regions were captured per retina for analyzing.